Ore Geology Reviews 89 (2017) 594–608

Contents lists available at ScienceDirect

Ore Geology Reviews

journal homepage: www.elsevier.com/locate/oregeo

Intracontinental rift-related deposits: A review of key models

Eduardo O. Zappettini [a,*], Nora Rubinstein [b], Sabrina Crosta [c], Susana J. Segal [a]

[a] Instituto de Geología y Recursos Minerales, SEGEMAR, Avenida General Paz 5445, San Martín, provincia de Buenos Aires, Argentina
[b] Consejo Nacional de Investigaciones Científicas y Técnicas (CONICET), Universidad de Buenos Aires, Departamento de Ciencias Geológicas, Pabellón II, Ciudad Universitaria, Buenos Aires, Argentina
[c] Instituto de Ciencias Polares, Ambiente y Recursos Naturales, Universidad Nacional de Tierra del Fuego, Argentina

ARTICLE INFO

Article history:
Received 17 May 2016
Received in revised form 13 June 2017
Accepted 16 June 2017
Available online 20 June 2017

Keywords:
Rift-related mineralizations
Detachment zones
Deposit models
Fluids characteristics
Source of metals and anions
Metallogenic model

ABSTRACT

Mineral systems associated with extensional fault systems in continental environments and not related to magmatic activity involve various deposit models that can be grouped into a single system which would plausibly explain the source and chemical composition of fluids, the formation depth, the source of heat and the structural history within a common geologic setting.

Mineral deposits related to this tectonic setting are those described within the detachment-related model, including massive replacements, stockworks and veins of Cu and Fe oxides (with or without Au), polymetallic sulfide veins, barite and/or fluorite veins and stratabound and vein Mn deposits. This paper reviews the abovementioned deposits as well as others related to this tectonic setting, such as Se-rich polymetallic deposits, Almadén type Hg deposits, U-Ni-Co-As-Ag polymetallic deposits with subordinated Bi-Cu-Pb-Zn (five element deposits), simple polymetallic Pb-Ag-Zn deposits, and the members of the IOCG clan (including the Au-Ag detachment-related deposits) involved in the Cu-Fe (-Au) model deposits.

All these mineral deposits are the result of fluid motion unrelated to magmatism in areas of thermal anomalies. These fluids collect certain elements producing a district mineralogical specialization with inhomogeneities in the distribution of mineralization types along the region affected by rifting. Fluid homogenization temperatures and salinities range between 60° and 430 °C, and 0 and 27 equivalent wt% NaCl, respectively. The O, S and D isotope composition is consistent with basinal poral fluids derived from meteoric waters under different P-T conditions in an active faults environment. Pb isotopes suggest that Pb derives from a mixture of rocks with a long period of residence in the upper crust and rocks deformed along repeated orogenic cycles with a contribution of Pb from the lower crust and even the mantle. Fluid flow along fault planes leads to different types of hydrothermal alterations depending on P-T conditions, particularly propylitization and low temperature potassium metasomatism.

All such deposits can be found in two different geotectonic environments of metallogenic interest involving extensional faults associated with detachment zones in depth; *i.e.*, 1) continental extension in a back-arc environment and 2) extension with rift development and generation of oceanic crust in a passive continental margin. Although the economic importance of this group of deposits is mainly related to industrial minerals, non-magmatic IOCG deposits could significantly augment the economic potential of this setting. The rift setting itself, without relation to detachments, is favorable for concentrating metals in stratabound deposits such as SEDEX ores. Additionally, the development of deposits directly related to magmatic activity contributes to the economic interest of this environment.

1. Introduction

Mineral systems associated with extensional fault structures in continental environments but unrelated to magmatic activity had not been previously differentiated from other low temperature mineralization. It was only recently that these mineral systems were recognized and individualized as specific genetic models. A group of such deposits was clustered by the U.S. Geological Survey under the model of "detachment-related mineralizations" Long, 1992a,b). This mineralization model was originally proposed to group various deposit types from Arizona, southeastern California and southern Nevada (USA) hosted by detachment and normal faults. This model involves Fe and Cu oxide massive replacements,

* Corresponding author.
E-mail address: eduardo.zappettini@segemar.gov.ar (E.O. Zappettini).

http://dx.doi.org/10.1016/j.oregeorev.2017.06.019
0169-1368/

stockworks and veins locally abundant in sulfides, as well as veins of barite and/or fluorite, and veins of Mn oxides (Spencer and Welty, 1986). This model also includes lacustrine bedded Mn oxide deposits and the associated low temperature Mn oxide veins, both of which are hosted in sedimentary rocks and deposited in half-graben basins. The associated hydrothermal alteration, which may or may not be present, includes chloritization of the footwall mylonitic rocks and K-feldspar replacement of the upper-plate rocks. The chloritic alteration is associated with sulfide mineralization and interpreted to be the result of retrograde metamorphism during the ascent of the hot lower-plate rocks to shallower depths. Low temperature K-alteration is associated to oxide mineralization and related to the upward circulation of saline brines derived from syntectonic basins along the detachment fault into normal faults of the upper plate. The fluid movement may have been driven by heat derived from either lower-plate rocks or syntectonic magmatism.

The aim of this paper is to analyze the various types of hydrothermal deposits in extensional environments and unrelated to magmatic activity in order to:

- Complete and broaden the typology of mineral deposits from extensional environments suggested by Long (1992a,b).
- Propose a new regional metallogenic model to serve as a basis for analyzing the potential mining areas affected by rifting and guide exploration from the perspective of the metallotects.

To achieve these objectives, we herein analyze the mineralizations related to rifting at a global scale in order to establish a generalized regional model regarding the physicochemical characteristics of the mineralizing fluids and the origin of the chemical elements.

2. Mineralization models related to faults in a rift environment

The reconnaissance of mineral deposits formed within an extensional environment but unrelated to magmatic activity led to the definition of the detachment-related mineralization deposits model proposed by Long (1992a,b) involving Mn bedded and vein deposits, Ba-F veins, and Cu-Fe-Pb-Ag-Au replacement and vein deposits. Other deposits not considered in this classification but formed in the same geological and tectonic setting were identified as separate models, *i.e.* polymetallic deposits of U-Ni-Co-As-Ag with subordinated Bi-Cu-Pb-Zn also known as five-element veins (Lefebure, 1996), Se-rich polymetallic deposits and the Pb-Ag-Zn simple veins (Beaudoin and Sangster, 1992).

The general characteristics and examples of the major districts at a global scale of the abovementioned deposits are hereafter described. The location of these deposits and the main rift zones of the word are illustrated in Fig. 1 and those of Argentina in particular are depicted in Fig. 2.

2.1. Deposit models

2.1.1. Mn deposits

Deposits of Mn related to detachment faults and the associated structures (Long, 1992a,b) are characterized by propylitic alteration, brecciation associated with veins, and the presence of extensive potassium metasomatism generally preceding the formation of the deposits and not always spatially associated with the mineralization. The mineralization usually occurs in the form of veins, although stratabound deposits hosted in sin-rift sedimentary sequences are also observed.

The general formation mechanism of these deposits was summarized by Spencer (1991), who suggested that the hydrothermal fluids associated with ore deposits at detachment levels retain Mn because of their acidic properties. Neutralization of these fluids by interaction with meteoric water results in the subsequent deposition of Mn with a characteristic mineralogy of highly oxidizing environments. Mn is deposited directly into unconsolidated sediments or veins near the surface. Ba, Pb, K and Sr anomalies are frequent within the ore, while the elements characteristically associated with epithermal systems linked to magmatism (As, Sb, Hg, Tl) occur in very low proportions and typically within the range of the geochemical background (Derby, 2012).

The stratiform deposits reach several hundred meters in length while generally not exceeding 20 meters in thickness. The mineralogy includes psilomelane, romanechite, potassium cryptomelane, ramsdellite and pyrolusite. Mn grades are low, usually between 4 and 14%.

The vein-type deposits present grades of up to 40% Mn but of reduced tonnage compared with stratiform deposits. When Mn veins are hosted in stratified rocks, they are usually associated with stratiform deposits. The mineralogy includes cryptomelane, hollandite, coronadite, psilomelane, romanechite and ramsdellite. The main gangue minerals are calcite and chalcedony/opal whereas barite veinlets can also be found. It should be noted that this type of mineralization does not at deeper levels change into

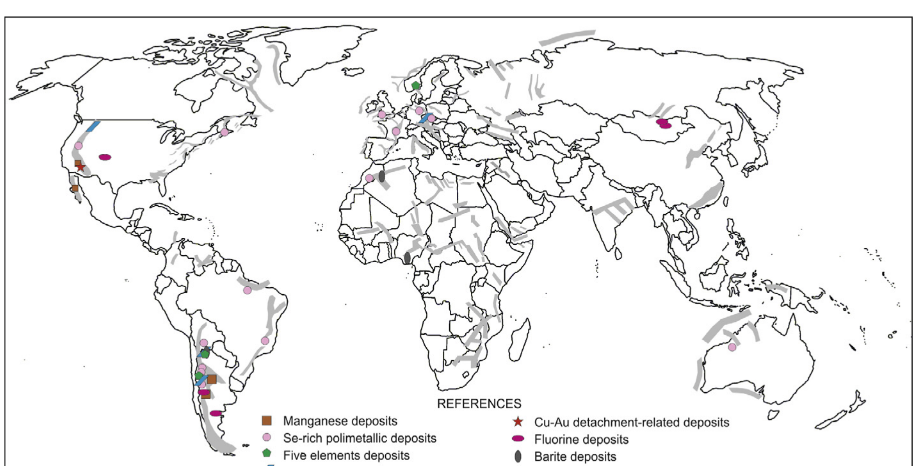

Fig. 1. Location of mineral deposits mentioned in the text and in grey the main Mesozoic rift systems of the world (Masson and Miles, 1983; Milanovsky, 1983; Gilder et al., 1991; Guiraud, 1998; Drake, 2005; Ziegler and Dèzes, 2006; Robertson, 2007; Roberts and Bally, 2012).

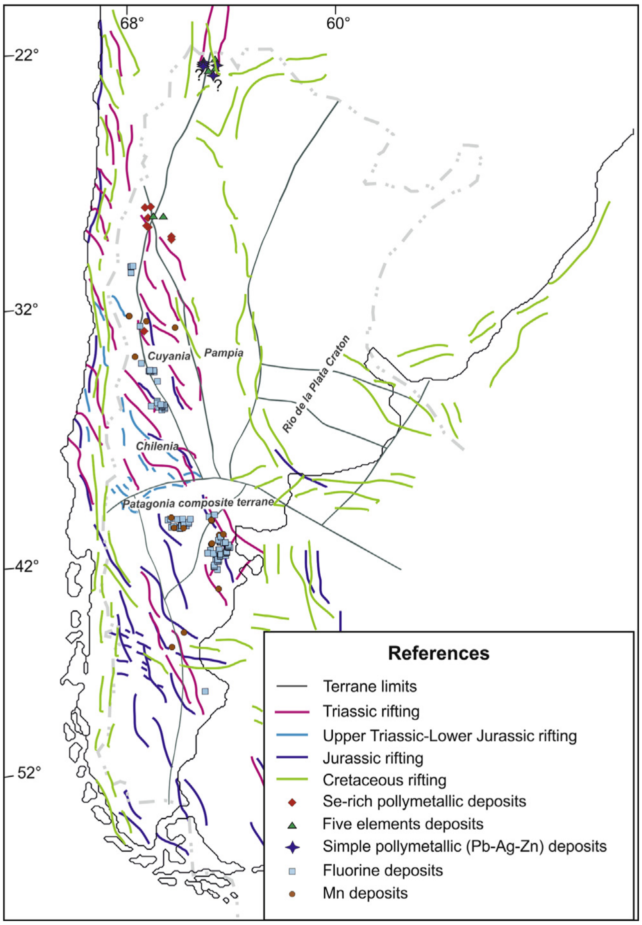

Fig. 2. Location of mineral deposits and their relationship with rift structures in Argentina.

a paragenesis typical of reducing environments (rhodochrosite), as is the case of the epithermal systems linked to continental volcanic arc environments. In contrast, the disappearance of the Mn assemblages, which are replaced by Fe oxides together with quartz and occasionally fluorite and barite, is observed (e.g., Leal et al., 2008).

The presence of alkaline basalts underlying Mn deposits is common and, locally, they can be channeled through faults and remobilize stratiform mineralizations (Derby, 2012). Examples of this type of deposit are District Artillery Park, Arizona, USA (Derby, 2012); Santa Rosa, Mexico (Rodríguez-Díaz et al., 2013); Sierra de Ambargasta, Argentina (Leal et al., 2008); and San Rafael Massif, Argentina (Mallimacci et al., 2010).

The Mn deposits from Sierra de Ambargasta, hosted in Proterozoic granites and rhyodacites, were partially mined from the early 1900's until 1980 and produced ~450,000 t of Mn (Leal et al., 2008). Such deposits include ~90 veins controlled by a dextral shear system related to N–S lineaments resulting from the breaking up of Gondwana. The ore paragenesis consists of hollandite, pyrolusite, ramsdellite, romanèchite and cryptomelane with massive, breccia, botroydal and drussy textures. The gangue minerals are goethite, hematite, calcite, opal, barite, and minor fluorite, quartz and chalcedony. Geochemical anomalies in Pb, Cu and particularly Au can be occasionally identified. Pervasive alteration affects the host rocks with an assemblage of opal, quartz and adularia along with minor calcite and epidote close to the contact with the veins. Outward, this assemblage grades to a white mica-chlorite alteration (Leal et al., 2008). Fluid-inclusion studies reveal that the mineralizing fluids had low temperatures (<150 °C) and salinities (<5 equivalent wt% NaCl) whereas isotopic data ($\delta^{13}C$, $\delta^{18}O$ and $\delta^{34}S$) on gangue minerals are consistent with a dominant meteoric source (Leal et al., 2008). K/Ar dating of cryptomelane yields a Lower Cretaceous age for the mineralization (134.5 ± 3 Ma, Brodtkorb and Etcheverry, 2000) with Mn probably sourced by basic magmatism linked with the breaking up of Gondwana (Leal et al., 2008).

The Mn deposits from the San Rafael Massif are hosted in the upper section of the Gondwanan volcanic sequence known as the Choiyoi Magmatic Cycle. The lower section of this sequence (Early Permian) exhibits geochemical features typical of a magmatic arc setting whereas the upper section (Late Permian) displays transitional geochemical characteristics between subduction and continental intraplate settings (Kleiman and Japas, 2009 and references therein). These Mn deposits were partially mined between the 1950's and the 1970's, with ore between 21% and 45% of Mn and calculated total reserves of ~390,000 t (Mallimacci et al., 2010). The ore bodies are tabular and lenticular with a length of up to 600 m, a thickness of up to 7 m and mainly NW, NE and EW striking. They consist of psilomelane, criptomelane, hollandite, coronadite, pirolusite, and minor wad, jacobsite, manganite, groxthite, ramsdellite, todorokite, hausmannite and calcofanite with massive, crustiform, colloform and breccia textures. The gangue minerals are Fe oxides, calcite, opal, chalcedony and quartz. Significant geochemical anomalies in Pb, Zn and Mo can be frequently identified. In the contact with the veins, the host rocks present pervasive argillitization and silicification with scarce disseminated pyrite and quartz veinlets (Malvicini and Delpino, 1989; Mallimacci et al., 2010).

Based on K-Ar dating, we have previously defined two episodes of Mn mineralization, an Upper Cretaceous and a Lower Miocene one, with the Mn derived from deep sources and the upper section of the Choiyoi Magmatic Cycle (Rubinstein and Zappettini, 2015). In that study, we argued that the Upper Cretaceous mineralization stage is genetically linked to the Triassic rifting that followed the extensional collapse of the Choiyoi Magmatic Cycle (represented by the upper section) and remained active until the Upper Cretaceous, while the Miocene stage is associated with an Early Miocene back-arc extensional regime related to the change in the subduction parameters in the Central Andes.

2.1.2. Se-rich polymetallic deposits

This group includes two subtypes (Simon et al., 1997): veins with Se, U, Cu, Co and Ni, and veins with Se, Au and EGP.

The first subtype consists of Cu, Co and Ni selenides and uraninite veins which are formed by oxidizing hydrothermal fluids. The typical example is Niederschlema - Alberoda, Germany. This deposit was formed during the Jurassic, when oxidizing hydrothermal solutions altered Permian uranium veins hosted in Variscan granitoids and introduced Mg, Se, Pb, Cu and Ag leached from the metamorphic host rocks. During the Cretaceous, a new paragenesis including native metals, Co-Ni-Fe arsenides and Bi sulfides was originated by partial dissolution and replacement (Förster et al., 2003, 2004).

Another example is the Rožná deposit, Czech Republic, which was formed in multiple episodes and is characterized by significant pre-mineralization hematitization originated by circulation of deep oxidants supercritical fluids and the presence of basinal brines. The mineralization is associated with the formation of transtensional grabens in the Bohemian Massif (Pešek et al. 2001) and was remobilized as a result of the initial stage of rifting in the region of Tethys-Central Atlantic during the mid to upper Triassic. Fluid circulation was controlled by pressure and temperature gradients in the initial stage of the graben formation and ceased due to tectonic inversion (Kríbek et al., 2009).

Other examples include Champagne, France (Johan et al., 1982); Otish Mountains, Canada (Johan et al., 1987); Kitka River Valley, Finland (Vuorelaine et al., 1964); Santa Brigida, Argentina (Brodtkorb, 1999); and Talampaya, Argentina (Zappettini et al., 2015).

The Santa Brigida deposit, with 0.036 Mt of 0.064% U, is hosted in Ordovician metamorphites affected by weak propylitization. The ore paragenesis consists of pitchblende, bornite, chalcopyrite, umangite, clausthalite, tiemannite, onofrite, eukairite, gold, silver and fischesserite along with secondary covellite, idaite, berzelianite, native Se and secondary uranium minerals (Brodtkorb, 1999). The Talampaya deposit includes 9 veins with predominantly NW-SE and subordinate NS strikes and hosted in Ordovician-Silurian granites. They mainly consist of barite and fluorite with minor Se and Cu minerals including umangite, klockmannite and clausthalite (Zappettini et al., 2015). Although there are not stratigraphic or isotopic constrains for the age of these deposits, they are preliminarly included within this model based on their mineralogy.

Vikre (2005) described Ag-rich deposits with Se in mining districts from the northern sector of the Great Basin, USA. The deposits were formed c.16–14.5 Ma, at a time of extensional tectonics and the development of bimodal volcanism (basalt-rhyolite). The paragenesis consists of Ag selenides (naumannite, aguilarite), Pb-Sb-Hg-Cu selenides (tiemannite, clausthalite, antimonselite, berzelianite) and native selenium, and frequently occurs near the surface and in association with sinters. The selenides can be found in association with sulfates in relatively oxidized thermal deposits where sulfides, except for cinnabar, are unstable. A high thermal gradient and Se/S ratio in the cooled hydrothermal fluid facilitate the transport of significant amounts of Ag, Au and other metals towards the paleosurface. Apparently, such transport occurs in the form of complex selenides, as suggested by fluid inclusion microthermometry and S isotope fractionation. Although the subsequent depression of the water table caused fluid boiling, H_2S exsolution and oxidation into H_2SO_4, the leaching of sinter and volcaniclastic deposits, and the widespread formation of alunite, primary selenides were preserved (Vikre, 2005).

In Argentina, in the area of Cerro Cacheuta, there is an Ag-Se deposit hosted in the synrift sequence of the Cuyo Basin, which locally consists of Middle-Upper Triassic continental sedimentary and volcaniclastic deposits and Middle Triassic basalts (Ramos and Kay, 1991; Spalletti et al., 2008). The deposit is made up of irregular and discontinuous veinlets of up to 4 cm in thickness with an ore paragenesis of naumannite, umangite, eskebornite, klockmannite, clausthalite, krutaite, bornhardtite-tyrrelite and trogtalite (Brodtkorb and Paar, 2013). Based on the geological setting, this mineralization could be genetically linked to the Mesozoic rifting.

Veins with Se, Au and EGP were usually referred to as apomagmatic or telethermal veins given that they are often hosted in sedimentary rocks of various ages and with no apparent connection to igneous bodies. Lindgren (1928) referred to them as belonging to the Au-selenides deposits to differentiate them from those deposits which contain sulfides. Simon et al. (1997) grouped such deposits into the selenide telethermal veins model.

In general, these deposits, which usually are of no economic interest, consist of small veins or veinlets of carbonate (±quartz, barite) with abundant hematite, selenides of Cu, Co, Ni, Pb, Hg and EGP, a few sulfides, and Au and EGP, especially palladium. The characteristics of the mineralizing fluids and the precipitation conditions were described by Shepherd et al. (2005). The mineralogical association indicates precipitation from oxidized fluids or brines with high chloride content. Conditions of low temperature, low pH, high fO_2 and high levels of chlorides favor the transport of Au and PGE as chlorinated complexes. The precipitation of these metals is related to the destabilization of the chlorinated complexes by the mixing with calcium-rich fluids, the dilution with meteoric waters or the interaction with reducing lithologies. The genesis of the Trogtal and Tilkerode deposits, Germany, has been associated with a mixture of reducing and oxidizing basinal brines (Cabral et al., 2012) in a Permo-Triassic rift-related basin environment (Shepherd et al., 2005).

Examples of this subtype of Se-rich polymetallic deposits are the aforementioned Tilkerode (Tischendorf, 1959; Wallis, 1994) and Trogtal (Ramdohr and Schmitt, 1955; Cabral et al., 2012) deposits, Germany; Caué (Clark et al., 1974; Cabral and Lehmann, 2007) and Serra Pelada (Cabral et al., 2002; Cabral and Lehmann, 2007; Grainger et al., 2008), Brazil; Copper Hills, Australia (Nickel, 2002); Bleïda Far West, Morocco (El Ghorfi et al., 2006); Hope's Nose, England (Stanley et al., 1990); El Dragón, Bolivia (Grundmann et al., 1990); and Cerro Cacho and Los Llantenes, Argentina (Brodtkorb and Crosta, 2010).

Cerro Cacho is hosted in a sequence composed of a Grenvillian basement intruded by carboniferous granites and pegmatites overlain by carboniferous sedimentary deposits which in turn are intruded by Middle to Upper Triassic dolerites (228 ± 5 and 223 ± 4 Ma, Fauqué and Caminos, 2006). The ore occurs in the form of thin veinlets of up to 30 mm of thickness hosted in calcite veins of a thickness between 50 and 300 mm and NE to EW striking. The ore paragenesis mainly consists of umangite, klockmannite, tiemannite, eucairite and clausthalite along with Cu-sulfides (chalcopyrite, bornite, chalcocite, digenite and idaite) in a calcite gangue. Locally, berzelianite, ferroselite, eskebornite, naumannite, tyrrellite, trogtalitakrutaite-penroseite, bellidoite, crookesite, chameanite, bukovite, cadmoselite, hakite, brodtkorbite, merenskyite, gold and fischesserite can also be found. Supergene processes produced azurite, malachite, calcomenite, schmiederite, atacamite and paraatacamite, and Fe-oxides (see Brodtkorb and Crosta, 2010 and references therein).

Los Llantenes deposit, primarily hosted in Ordovician metamorphic rocks, was mined for Hg during a short time in the 1960's and 1600 kg of this metal were obtained. The deposit consists of veinlets some centimeters thick and some tens of meters long, located in ENE-WSW and NE-SW faults (Brodtkorb, 1999). The hypogene ore paragenesis is complex and includes bornite, chalcopyrite, cinnabar and metacinnabar, umangite, tiemannite, clausthalite, eukairite, eskebornite, stilleite, naumannite, klockmannite, onofrite, ferroselite, fischesserite, berzelianite, onofrite, aguilarite, chrysstanleyita, jagueite and native Au and Hg-bearing silver in a calcite with minor quartz and barite gangue. In addition to Cu carbonates, sulfates, oxides and halides, and Fe oxides, the supergene assemblage comprises the Se minerals schmiederite, chalcomenite and molybdomenite as well as native Se (Brodtkorb and Crosta, 2010 and references therein). New field work and petrological data reveal that this mineralization is also hosted in Middle to Upper Triassic alkaline hypabyssal gabbros that intrude the Ordovician metamorphic rocks. Besides, the RREE pattern of the ore samples is very similar to that of the gabbros, thus suggesting a common source for the magmatism and the mineralizing fluids which allows assigning a Triassic age to these Se deposits (Zappettini et al., 2015).

2.1.3. U-Ni-Co-As-Ag polymetallic deposits with subordinated Bi-Cu-Pb-Zn (five-element veins)

According to Lefebure (1996), the deposits assigned to this model are related to hydrothermal systems in which fluids ascend along faults developed in a crustal extension setting, depositing metals 1 to 4 km deep. The fluids are brines with temperatures between 150 °C and 250 °C, which originated both in the later stages of the magmas differentiation and in relation with convective flow of water in country rocks. The source of metals could be sulfides-rich stratigraphic levels and carbonaceous shales interbedded in the stratigraphic sequence.

The geotectonic setting corresponds to an intracratonic rift or traction-elongation zone of back-arc developed in a continental crust in which deposits are often post-tectonic (Lefebure, 1996). Kissin (1992) proposed a general genetic model in which, in a rift environment, an anomalous heat flow generates temperatures of around 400 °C 10 km deep. These conditions favor the mobilization of formational brines and other connate waters that migrate along the extensional faults. High salinity and temperatures favor the migration of Co, Ni and Ag. The mineralogical variations result from changes in the redox conditions and a mixing with meteoric water.

These deposits are characterized by open space filling textures and a complex paragenetic association which includes Ni-Co arsenides, Co, Ni, Fe and Sb sulfarsenide, Bi and Ag sulfides and uraninite, and, more rarely, Au. In some deposits, uraninite proves of economic interest (Lefebure, 1996).

Examples of such deposits are Cobalt, Ontario, Canada (Berry and Petruk, 1971); Kongsberg-Modum, Norway (Bjerkgård, 2012); Purísima-Rumicruz (López, 2011); and Carrizal, Argentina (Morello and Rubinstein, 1997).

The Purísima-Rumicruz deposit, hosted in Ordovician platform sedimentary rocks, was mined between the 1940's and the 1970's for barite, Pb and Cu and thereafter sporadically explored by different mining companies. Its average Cu grade is of 4% while that of Pb ranges from 1% to 7%, that of Ni, between 0.01% and 0.3%, and, for Ag, the grade reaches up to 270 ppm. The mineralization occurs in the form of veins of up to 0.5 m of thickness, usually with breccia texture and with WNW and subordinate EW and NS strikes. The ore paragenesis, which underwent an important supergene alteration, includes galena, pyrite, chalcopyrite, Zn-bearing tetrahedrite-tenantite, chalcosite, nickelite, gersdorffite and Co-gersdorffite, ullmanite, pitchblende, bornite, digenite, and millerite. The gangue mainly consists of calcite with minor ankerite, dolomite and siderite, variable barite and scarce quartz. Fluid inclusion studies conducted in quartz indicate that the mineralizing fluids had temperatures of between 150 °C and 250 °C, and salinities between 5 and 12 equivalent wt% NaCl, whereas isotopic data ($\delta^{13}C$, $\delta^{18}O$ and $\delta^{34}S$) reveal a sedimentary/metamorphic source (López, 2011). Based on a Pb/Pb model age of 235 Ma in sulfides and considering the dispersion of the isotopic data and the mineralization structural controls consistent with an extensional tectonic regime associated with the Mesozoic rifting in northwestern Argentina, Lopez (2011) suggested a Jurassic- Lower Cretaceous age for this five-element type mineralization, with the Pb sourced by the Ordovician host rocks.

The Carrizal deposit is hosted in continental sedimentary rocks of Carboniferous age intruded by Permian Choiyoi Magmatic Cycle volcanics. The mineralization occurs mainly in the form of blind veins with NS striking, breccia texture and ore grades between 0.02% and 0.7% U_3O_8. The ore paragenesis consists mainly of rammelsbergite, gersdorffite, hypogene anabergite and pitchblende along with subordinate pyrite, niquelite and bismutite with scarce dolomite gangue. The sedimentary host rocks exhibit pervasive and veinlet-type carbonatization. The chemical composition of gersdorffite suggests formation temperatures of between 200 °C and 300 °C (Morello and Rubinstein, 1997). Crystallographic parameter data of pitchblende obtained by Morello and Rubinstein (1997) suggest an Upper Triassic age (~205 Ma) which enabled the linking of this mineralization with the extensional tectonic regime that prevailed in Southwest Gondwana during the Mesozoic.

Simple U veins linked to rifting settings may also be included within such model, as is the case of the Las Termas deposit in Argentina. This deposit, which has been explored by the Comisión Nacional de Energía Atómica (Argentina) since the 1980's, bears U contents of between 0.1% and 9.2% U_3O_8. It consists of veins composed of pitchblende and pyrite in a fluorite gangue which are hosted in a Lower Paleozoic metamorphic basement intruded by alkaline basalts of ~130 Ma. An U/Pb dating on pitchblende returned an age of 113,6 ± 3,2 Ma, which falls within the age range of the alkaline magmatism genetically tied to the Mesozoic rifting in northwestern Argentina (Morello et al., 2011).

2.1.4. Simple Pb-Ag-Zn deposits

These deposits include veins of base metals (Pb-Zn-Ag) hosted in clastic metasedimentary sequences (Beaudoin and Sangster, 1992). Such veins are associated with subsidiary fault zones related to major crustal faults and located in orogenic environments with or without the presence of arc magmatism. They are late-tectonic and associated with extensional settings where the thinning of the crust and the rise of the upper mantle occurs. Consequently, a thermal disequilibrium as well as the generation of deep fractures and block rotation leading to fluid convection occurs. In this model, the deep crustal fault zones are considered first-order channels for the circulation of hydrothermal fluids, which connect deep with shallow reservoirs leading to a mixture of sources for Pb, S and fluid which is reflected in the isotopic characteristics of the minerals (Beaudoin and Sangster, 1992). The role of metamorphism is related to the generation of fluids by dehydration or water/rock exchange at high temperature. The ore paragenesis consists of galena and sphalerite along with minor pyrite, chalcopyrite and silver sulfosalts whereas the gangue minerals include siderite, quartz, dolomite and calcite. Pb/(Pb + Zn) ratios range from 0.51 to 0.72 and Au is usually absent or present in very low contents.

Beaudoin and Sangster (1992) emphasized the presence of other vein-type mineral systems associated with this model in some of the districts studied and cited the presence of F-Ba and "five-element" veins in the Freiberg district but ruled out a link between them.

Examples of simple Pb-Ag-Zn deposits are Coeur d'Alene, USA. (Bennett and Venkatakrishnan, 1982); Pribram, Czech Republic (Beaudoin and Sangster, 1992); Pumahuasi (Segal et al., 1999), Paramillos de Uspallata (Carrasquero et al., 2013) and Castaño Viejo (Cardó, 1999), Argentina.

The Pumahuasi deposit, which is hosted in Ordovician metamorphic rocks overlain by Cretacic sedimentary rift deposit, was mined during the early twentieth century with ore grades between 8% and 35% of Pb and Zn and between 53 g/t and 100 g/t of Ag, and total reserves of 0.15 Mt (Segal et al., 1999 and references therein). The mineralization occurs in the form of veins of up to 0.4 m of thickness and with predominantly EW strike hosted in a NNW-SSE shear belt that forms part of a sinistral Riedel system. The ore paragenesis includes galena, sphalerite, chalcopyrite, arsenopyrite, tetrahedrite-tennantite, covellite and digenite and the gangue consists of a quartz, barite and siderite. S and Pb isotope data suggest that the S was leached from the local country rock by circulating waters, whereas the Pb derives from the upper crust and rocks formed during repeated orogenic cycles (Segal et al., 1999). According to the stratigraphic controls, this deposit would have formed between the Silurian and the Jurassic; however, the similarity between the Pb isotope data and those of the Purísima-Rumicruz deposit would enable the constraining of the age to the Triassic-Jurassic (Zappettini et al., 2015).

Castaño Viejo was sporadically mined and explored between the 1860's and the 1980's, with ore grades between 3% and 9% of Pb, of up to 7.4% of Zn, between 114 g/t to 507 g/t of Ag and of up to 2 g/t of Au, and total reserves of 800,000 t (Cardó, 1999 and references therein). The deposit includes ~ 30 veins with predominantly E-W strike and hosted in the Permian Choiyoi Magmatic

Cycle volcanics. The veins are of up to ~1 m of thickness and of up to ~500 m of length and display banded, drusy and rarely breccias textures. The ore paragenesis consists mainly of sphalerite, Ag-galena, pyrite and chalcopyrite along with minor chalcocite and tetrahedrite in a quartz and carbonate (calcite and siderite) gangue. Supergene processes produced scarce anglesite, cerusite, goslarite, malachite, azurite, calcantite and limonites along with secondary chalcocite and covellite (Cardó, 1999). K/Ar dating on the subvolcanic host rock yielded a Middle Triassic age (237 ± 12 Ma) which enables the linking of this mineralization with the Mesozoic rifting of Southwest Gondwana.

The Paramillos de Uspallata deposit includes thirty-three veins hosted in the Mesozoic synrift volcano-sedimentary sequence of the Cuyo Basin. This deposit was discontinuously mined from the seventeenth century until the early 1980s and produced nearly 414.000t of ore at ~2.5% Pb, 3.5% Zn and 475 g/t Ag. The veins are of up to ~2 m of thickness and of up to ~2500 m of length and display crustiform, cockade and breccias textures and predominantly NW and WNW and subordinate WSW strikes. The paragenetic sequence consists of a galena and sphalerite intergrowth, minor chalcopyrite and scarce pyrite in a siderite with minor quartz gangue. These sulfides are variably replaced by freibergite which in turn is variably replaced by boulangerite and owyheeite. This sequence ends with arsenopyrite and marcasite in a quartz gangue. Wall-rock alteration surrounding the veins includes pervasive sericitization and carbonatization and veinlet-type silicification (Carrasquero et al., 2013). Fluid inclusion studies conducted in quartz, siderite and sphalerite show that the mineralizing fluids had low temperatures (between 160° and 250 °C) and moderate salinities (5 to 19 equivalent wt% NaCl), whereas the isotopic data ($\delta^{34}S$ and $\delta^{18}O$) obtained in sulfides, quartz and siderite suggest a mixture of magmatic and meteoric sources (Garrido et al., 2001). Pb isotopes obtained for galena not only are consistent with a mixture of sources typical of the simple Pb-Ag-Zn deposits but also plot in the "Mesozoic Array" line defined by Paiement et al. (2012), suggesting a link with the Cuyo Basin Mesozoic rifting (Zappettini et al. (2015).

2.1.5. Cu-Au deposits in detachment fault zones

This model (Long, 1992a,b) includes polymetallic deposits where the main ore consists of Cu and Au massive replacements, stockworks and veins in detachment fault zones. These deposits are characteristic of extensional environments and, at regional scale, are related to half-grabens and hydrographically closed basins syntectonic with the extensional deformation within the upper block of the detachment fault zone. The best-studied deposits related to this model are located in eastern California and southwestern Arizona, USA, and include the Bullard (Spencer and Reynolds, 1992), Northern Plomosa (Duncan, 1990) and Copperstone (Spencer et al., 1988) districts.

Detachment fault-controlled low-sulfidation gold mineralization can be considered a local variant of the Cu-Au deposits in detachment zones. Au mineralization is located in massive, tabular ore bodies above the detachment fault zone, and in open-space filling ores along listric faults. The ores are in zones with strong silicification and brecciation, which are synchronous with detachment faulting. Mineralization is composed exclusively of Au and electrum (with Au/Ag ~3), with traces of Au-Ag tellurides, arsenopyrite and galena, in a gangue of quartz and carbonates, similar to mesothermal Au veins. Alteration consists of quartz, adularia, chlorite, sericite, calcite, pyrite and clay minerals and isotopic data suggest the involvement of metamorphic fluids. Deposits of this type include Riverside Pass, in southeastern California, USA (Wilkinson et al., 1988), Ada Tepe, in Bulgaria (Marchev et al., 2004), and Ernesto-Lavrinha, in the Guapore Gold Belt, Brazil (Puritch et al., 2016). Sr isotope data from the Ada Tepe deposit reveal a metamorphic origin for hydrothermal fluids, which is consistent with the available Pb isotope data; however, a contribution from an igneous source is not ruled out.

The Cu-Au detachment deposit model is interpreted as a representative of the Iron Oxide Copper Gold (IOCG) clan related to fluids of evaporitic origin (Barton, 2014). Indeed, the IOCG clan includes various deposit types that share similar features, such as hypogene magnetite and/or hematite, scarcity of sulfides and enrichment in a suite of distinctive minor elements (P-F-Co-Ni-V-Cr-As-Ag-U-REE), although varying considerably in form, size, and degrees of enrichment. Notably, some IOCG deposits are associated with distal Co–Ag–As– (Ni–U) veins (e.g., Great Bear, Mumin et al., 2007). IOCG type mineralizations can be hosted in various tectonic settings although shallow- to mid-crustal intracratonic, intra-arc or back-arc continental extensional settings, as well as late- or post-orogenic settings are the most prospective. Some of these types of mineralizations lack coeval magmatism and this group includes the Cu-Au detachment-related deposits. Although Cu-Au deposits in detachment fault zones contain relatively little magnetite and high-temperature alteration, they share some characteristics with the IOCG clan, such as low-temperature K-metasomatism and hematite-rich mineralization (Barton, 2014).

The non-magmatic IOCG end member is associated with evaporitic fluids mobilized by deeper-seated intrusions, which drive a hydrothermal convection cell. However, in this sub-model, an alternative genetic scenario involves metamorphic-hydrothermal fluids derived from distinctive crustal sources (involving a meta-evaporitic or mantle source for the Cl/F with regional plumbing) by metamorphic devolatilization and water–rock interaction at depth (Barton, 2014).

The IOCG systems of Northwest Queensland include epigenetic mineralization consisting of small deposits located in intracontinental and continental environments (North Australian Craton) and larger deposits facing the passive continental margin affected by rifting. Most of these deposits were generated at the time of basin inversion and intrusion of mainly felsic magmas. Hot saline and oxidizing fluids of either magmatic or metamorphic origin are interpreted to be responsible for the transport of Cu and Au (Hutton et al., 2012). Characteristically, hydrothermal Cu ± Au mineralization overprints earlier Fe oxide concentrations of different origins, and K and Na-Ca alterations are common and usually widespread. In particular, the unusual Monakoff IOCG deposit (Williams et al., 2015), located to the northeast of Cloncurry within the Eastern Succession of the Mount Isa Inlier, is characterized by an enrichment in Co, Ag, As, Mn, REE, U, Pb, Zn and Sr, high concentrations of F and Ba and the overprinting of a late Co-As-Au-Bi mineralization. The mineralization, which is probably linked to granitic intrusions, results from the mixing of an oxidized F, Ba, REE and U-rich fluid with a reduced S-bearing fluid. Evidence of extension with associated K-enriched zones and U-rich zones has also been found (Austin et al., 2016). It is noteworthy that the Olympic Dam deposit occurs in an F-rich silicic large igneous province (McPhie et al., 2011).

IOCG deposits in the Andean region were emplaced in an extensional regime, but are greatly different from the tectonic setting considered herein. Moreover, a link with magmatism is evident and the participation of deeply derived magmatic fluids is favored; involvement of brines from external sources is unlikely, although their local participation cannot be precluded (Sillitoe, 2003). In Argentina, the most favorable regions for the targeting of this deposit model are the Mesozoic back-arc, and intracontinental extensional basins and the associated magmatism developed to the east of the Andes (Cuyania and Pampia terranes).

2.1.6. Almadén-type Hg deposits

The cinnabar from Almadén deposit is likely to have been mostly remobilized–crystallized during the regional extensional tectonic events, capturing Pb from the host sedimentary sequence, mobilized by large-scale, long-term hydrothermal convective cells (Palero-Fernández et al., 2015). Hg mineralization occurs in strata-bound and stockwork deposits consisting of cinnabar as a major phase, with minor pyrite and Hg and traces of quartz, dolomite-ankerite, barite and siderite. Hydrothermal alteration includes a proximal pyrophyllite-kaolinite-illite-quartz assemblage and distal (quartz)-illite-chlorite-(pyrophyllite) or rectorite-(chlorite) assemblages (Higueras et al., 1999). The alteration process also affected the alkaline mafic rocks of the region, resulting in an assemblage of Cr-illite, fuchsite, Cr- chlorite, dolomite (Morata et al., 2001), which can be considered a listwanite-type alteration. Total production at Almadén reached 7 Mt, averaging 3.5% Hg. Fluid inclusion studies conducted in quartz from the proximal alteration assemblage indicate low to moderate salinities (1 ± 13 equivalent wt% NaCl) and temperatures (150–375 °C, mode at 220 °C) and deposition depth of ~ 1.8 km (Higueras et al., 1999). The Pb isotope ratios are heterogeneous and are interpreted as representing Pb extraction during various events related to the main extensional or transtensional tectonic events (late Ordovician - Devonian, Permian - Triassic and Late Jurassic - Early Cretaceous) in the region (Higueras et al., 2005; Palero-Fernández et al. 2015).

2.1.7. Fluorite deposits

Fluorite-barite epigenetic vein deposits are the main source of fluorine worldwide. This model, which corresponds to veins hosted in breccias and shear zones along faults that are essentially located in tectonic environments underlain by sialic crust, was summarized by Hora (1996a). In orogenic belts, veins are related to post-tectonic intrusions or alkaline rocks associated with rifts located close to suture zones, tensional rifts, grabens and lineaments. The ore bodies are tabular or lenticular and may exceed 1000 m long, with thicknesses up to 20 m. In many cases, they are composed only of fluorite, but quartz, chalcedony, barite, Ca-Fe-Mg carbonates and minor sulfides, such as galena, sphalerite, chalcopyrite and pyrite, could also occur. Associated pervasive potassic alteration is common.

Typical examples of this deposit model are the districts located along the Rio Grande graben in western USA, which extends over 800 km, the Baikal rift zone in Russia and Mongolia, which extends over more than 1500 km (Mats and Perepelova, 2011; Zorin et al., 2003), and the San Rafael Massif (Rubinstein and Zappettini, 2015) and North Patagonian Massif (Aliotta 1999) districts in Argentina. In all cases, the mineralization is located within normal or *en échelon* faults, associated with rift systems.

Fluorite ore deposits from the San Rafael Massif are hosted in the upper section of a Gondwanan Choiyoi Magmatic Cycle (see Mn deposit from the San Rafael Massif). Some of these fluorite deposits were partially mined between the early 1940's and the early 1980's, with ore grades up to 90% CaF_2 and calculated total reserves of ~480,000 t (Centeno et al., 2009; Mallimacci et al., 2010 and references therein). The ore bodies are mainly lenticular and minor tabular with lengths of up to 900 m, thicknesses of up to 4 m and mainly NNW and E-W striking. The deposits consist of one or two generations of fluorite with colloform, crustiform, cockade and breccia textures. The paragenetic sequence begins with lattice-bladed calcite, and is followed by the first generation, which consists of coarse crystals of fluorite, and the second generation, which is composed of fine fluorite aggregates intergrown with minor quartz. Each fluorite generation is followed by a silicification stage that leads to quartz with typical epithermal textures. Scarce pyrite and arsenopyrite are sporadically recognized. Fluid inclusion studies conducted in fluorite from two different deposits have revealed that the mineralizing fluids had low temperature (~<200 °C) and low salinity (<2 equivalent wt% NaCl). In the host rocks, the fluorite veins develop pervasive argillization and silicification along with disseminated pyrite, interstitial fluorite and quartz veinlets (Rubinstein and Zappettini, 2015 and references therein). Based on a Sm/Nd isochrone age in fluorites (194–216 Ma) and geochemical data, we have previously argued that these fluorite deposits were formed during the Upper Triassic-Lower Jurassic as a result of the Triassic rifting that followed the extensional collapse of the Choiyoi Magmatic Cycle and triggered hydrothermal activity at regional scale in the San Rafael Massif, with the F derived from a mantle source and the REE from the upper section of the Choiyoi Magmatic Cycle (Rubinstein and Zappettini, 2015).

Fluorite deposits from the North Patagonian Massif are hosted in a thick Lower Triassic –Jurassic volcanic sequence (Marifil, Los Menucos and Garamilla Formations, see Ramos and Aguirre-Urreta, 2000). This sequence is part of the Mesozoic Patagonian Silicic Large Igneous Province that resulted from the crustal melting linked to the Gondwana breakup (Pankhurst et al., 2000) and, locally, is structurally characterized by half-graben systems (Cicciarelli, 1990). Some of these deposits were partially mined between the 1960's and the early 1980's, with total mineral resources of 8,161,000 t and an average F_2Ca grade between 30 and 50%. The systems consist of ~150 veins with lengths of up to 1600 m, thicknesses of up to 10 m and mainly E-W to N55°E striking. They are composed of fluorite, chalcedony, quartz and minor calcite; locally, barite, adularia, zeolites, rodocrosite and scarce sulfides (pyrite, galena, sphalerite and chalcopyrite) can also be found. In the host rocks, the fluorite veins develop pervasive sericitization and silicification and minor argillitization and zeolitization. Fluid inclusion studies have revealed that the mineralizing fluids had temperatures between 100 and 300 °C and salinities of up to 2 equivalent wt% NaCl (Aliotta, 1999 and references therein). According to Cicciarelli (1990), the vein emplacement is controlled by the half-graben system due to the extensional tectonic regime linked to the Gondwana breakup that also led to crustal thinning and triggered melting processes in the base of the crust, all of which resulting in an abundant rhyolitic magmatism whose late fluids would be responsible for the fluorite mineralization.

2.1.8. Barite vein deposits

This model includes veins consisting essentially of barite, hosted in faults, fractures and shear zones that fall within the general model of barite veins in various tectonic environments defined by Clark and Orris (1991). Hora (1996b) indicated that the veins tend to be located in and around the basin margins in both continental rift and continental margin settings. The mineralization is controlled by high-angle faults and, locally, it occurs as strata-bound and irregular bodies. The veins have an extension that can exceed 1 km, are up to 20 m thick and are exploited up to 500 meters deep.

The paragenesis comprises barite associated with quartz/chalcedony, with varying proportions of fluorite, calcite and sulfides such as sphalerite, chalcopyrite, galena and, rarely, silver sulfosalts. The presence of multiple episodes of mineralization is common (Hora, 1996b). Fluid inclusion studies (Jessey, 2010) have revealed homogenization temperatures between 160 and 300 °C and salinities between 10 and 16 equivalent wt% NaCl. Some of the characteristic districts belonging to this model are the Calico Mountains in California, USA (Jessey, 2010), the Benue Trough Basin in Nigeria (Oden, 2012) and Santa Victoria in Argentina (Castillo, 1999).

The Santa Victoria district, consisting of veins mainly composed of barite along with variable quartz and galena and accessory sphalerite, chalcopyrite and pyrite, is hosted in a Neoproterozoic to Ordovician sedimentary sequence. This district, partially mined in the 1980's, produced 20000 t of barite and has calculated total reserves of ~270,000 t (Castillo, 1999). Isotopic studies performed by Sangster (2001) have shown that the Pb was sourced by the deep Precambrian basement whereas the S derives from sulfides of the sedimentary sequence which ultimately result from marine sulfate reduction. Although there are no stratigraphic or isotopic constrains for the age of these deposits, based on their mineralogy and geological setting, similar to that of the Pb-Zn-Ag simple veins from the Pumahuasi district, they could be preliminary assigned to this model (Zappettini et al., 2015).

3. Characteristics of mineralizing fluids within rift environments

3.1. Overview

Conditions in a rift environment give rise to two mineralizing processes: (a) one caused by the movement of fluids unrelated to magmatism in areas of thermal anomalies and (b) another one related to magmatic activity. In the first case, where there is a favorable source, fluids collect certain elements, producing a mineralogical specialization at district scale with inhomogeneities in the distribution of mineralization types along the region affected by rifting.

Considering the model where a detachment fault separates a lower hot block from an upper cold block with the development of listric and flat normal faults, the forming mechanism of ore deposits involves a process of retrograde metamorphism in the lower hot block and the circulation of brines derived from syntectonic basins along detachment faults toward the normal faults affecting the upper block. Mineralization consists of sulfides or oxides, depending on the redox conditions. Fluid motion would be linked to the lower block heat or to the presence of syntectonic magmatism (Reynolds and Lister, 1987).

The isotopic and fluid inclusion data of the groups of deposits described above allow establishing the physicochemical conditions of the mineralizing fluids and defining their genesis and relationships between different subtypes.

3.2. Temperature and salinity

The data compiled from the publications previously cited for each deposit type described in Section 2.1. allow establishing the temperatures and salinity ranges that define a field (A in Fig. 3) delimited by homogenization temperatures ranging between 60° and 430 °C and salinities ranging between 0 and 27 equivalent wt% NaCl.

The characteristics and behavior of fluids in the detachment and direct faults environment have been analyzed by Reynolds and Lister (1987). According to these authors, the variations in the different types of mineralization are related to the presence of two fluid systems: a deep fluid system mobilized by convection in the deep parts of the shear zone and a fluid system in the upper block, where meteoric and connate water prevails at hydrostatic pressures. Movements in the detached zone juxtapose rocks affected by the different systems and allow their superposition.

According to the data presented by Baatarstog (2006) for fluorite, barite and Pb-Zn-Ag veins from the Schwarzwald district, Germany, the early fluids correspond to deep brines at temperatures ~350 °C, which, during their ascent, mixed with low-salinity waters. The mixture of both fluids would have been facilitated by an increase in the tectonic activity and resulted in the deposition of mineralization.

3.3. Isotopic characteristics

Overall, the O, S and D isotopes values (Table 1) are consistent with basinal poral fluids derived from meteoric waters under various P-T conditions in an environment of active faults.

$\delta^{34}S$ values indicate formational brines and progressive mixing with meteoric water. $\delta^{18}O$ and δD values are within the range of metamorphic and meteoric fluids, suggesting a progressive oxygen exchange related to fluid-rock interaction in the basement during

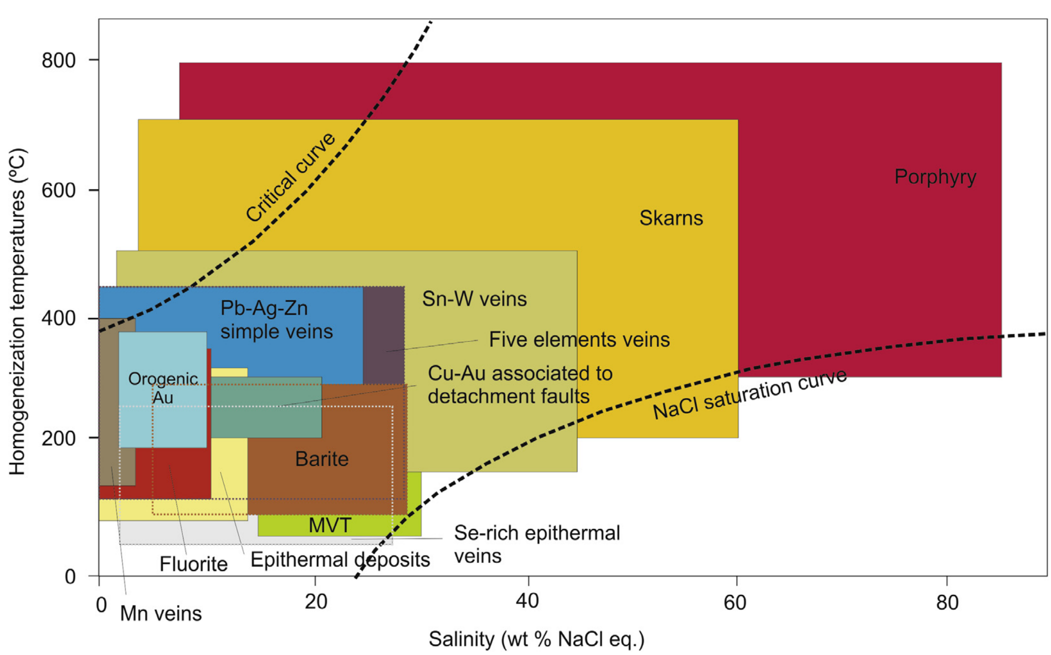

Fig. 3. Homogenization temperature vs salinity (% by weight NaCl eq.) diagram, showing the schematic distribution of the main deposit types considered in this work and other deposits models for comparison. The A field indicates the ranges of T and salinity fluids mineralization associated with rifting environment failures. Data from the sources cited in this publication, Constantopoulos (1988) and Wilkinson (2001).

Table 1
Isotopic characteristics of deposits associated with rifts.

Deposit model	δ18OSMOW ‰	δD ‰	δ34S ‰	References
Simple Pb-Ag-Zn veins	−5.5 to +20	...	+16 to +26	Beaudoin and Sangster (1992)
Barite veins	+12	−47 to −71	+12 to +27	Kontak et al. (2006) Sizaret et al. (2009) Canals and Cardellach (1996)
Fluorite veins	+10 to +30	−1 to −78	...	Sizaret et al. (2009) Baatarstog (2006)
Cu-Au in detachment-fault zones	−5 to +8	...	...	Roddy et al. (1988) Long (1992b)
Five elements veins	+0.5 to +26	+5 to −95	−22 to +20	Kissin (1992)
Se-rich polymetallic veins	+4 to +20	−39 a −89	−10 to +28	Kríbek et al. (2009)
Mn veins	+6 to +22	...	+5 a +8	Eggleston et al. (1983) Leal et al. (2008)

their ascent, considering that originally basinal brines correspond to meteoric or sea water (Baatarstog, 2006).

Pb isotopes are relatively homogeneous within each district but vary between them, suggesting different sources. In general, the data are grouped between the curves of the lower and upper crusts (Zartmann and Doe, 1981) in the uranogenic diagram (Fig. 4). This suggests that Pb derives from a mixture of rocks with a long period of residence in the upper crust and rocks deformed during repeated orogenic cycles (Beaudoin and Sangster, 1992), with a contribution of Pb from the lower crust and even from the mantle (Paiement et al., 2012). It is noteworthy that the isotopic data for all the mineralization considered are grouped following the "Mesozoic Array" defined by Paiement et al. (2012) for the Purcell Basin and Coeur d'Alene deposits, which is interpreted as the result of episodes of Pb isotopic mixture during the Mesozoic and even the Cenozoic. The Mesozoic Array is broad, which, according to these authors, responds to several sedimentary sources.

3.4. Associated hydrothermal alteration

The hydrothermal alteration caused by fluid flow along fault planes associated with detachment zones at different Eh, pH and P-T conditions has been described and summarized by Michalski et al. (2007) (Fig. 5). Rocks of the lower block are usually brecciated (up to 300 m below the detachment zone according to Long (1992b)) and affected by propylitic alteration (chlorite-epidote-calcite) caused by reducing hot fluids, whereas those of the upper block are affected by low temperature potassium metasomatism (ranging up to two kilometers above the detachment zone according to Long (1992b)) with an assemblage of adularia and K-enriched biotite, produced by hot oxidizing meteoric fluids. The hydrothermal alteration assemblages depend on the permeability and reactivity of the rocks involved. The release of chemical elements of interest (metals, Ba, etc) occurs in relation to the fluid flow and the consequent alteration of the rocks involved. In this case, the amount of metals released by this mechanism is enough to form mineral deposits without requiring a deep crustal source (Michalski et al., 2007). Table 2 shows the hydrothermal alteration types observed in various models of mineralization formed in this environment due to different P, T and redox conditions.

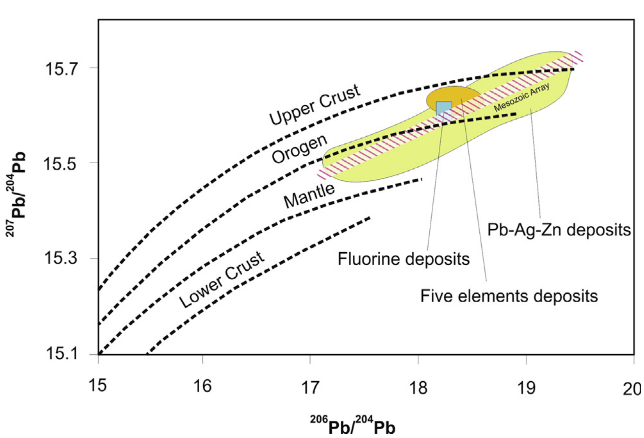

Fig. 4. Comparison of Pb isotopic compositions in various deposit models linked to extensional environments (data from Beaudoin and Sangster, 1992; Sizaret et al., 2009; López, 2011). The shape of the "Mesozoic Arrangement" modified from Paiement et al. (2012) is indicated.

Hydrothermal alteration assemblages cannot be individually differentiated from those related to hydrothermal fluids linked to magmatic activity. However, the lateral and in-depth regional distribution pattern allows their discrimination (cf. Fig. 5).

3.5. Sources of metals and anions

3.5.1. Base metals

Geochemical studies of marine shales indicate that they are generally enriched in metal elements and can be a source of metal-rich mineralizing fluids (e.g. Ruffell, 1998). For instance, the Ordovician marine basin sediments in northwestern Argentina are a potential source of metals for the five-element deposits in the region due to their high Ba, Cu, Ag, Pb, As, Ni, Co, Zn and U contents (López, 2011).

The Pb isotopes from districts of simple polymetallic Pb-Ag-Zn deposits suggest that this metal derived from the upper crust, and leached from sedimentary rocks, with variable contributions of the lower crust (Beaudoin and Sangster, 1992; Paiement et al., 2012). In the Pumahuasi and Santa Victoria districts, Argentina, Sangster (2001) came to a similar conclusion, strengthening the model of a crustal source for Pb without a link with magmatic activity.

3.5.2. Manganese and Iron

Mn is the second most abundant transition element on the earth's surface, where it is naturally mobile under oxidizing conditions. This mobility occurs in a wide range of temperatures and chemical environments, and can produce stratabound and vein-type deposits in which anomalous contents of Sr, Ba and As are common.

The Mn and Fe mineral systems and occurrences associated with rift environments with restricted development of sea basins have a volcanogenic origin related to bimodal magmatism. In the case of Mn veins formed in the absence of marine sequences (and thus without associated submarine hydrothermal activity), it has been interpreted that the source of Mn and Fe was the alkaline basic magmatism related to intracontinental rifting (e.g. Leal et al., 2008), or the country rocks from which they were leached (Rubinstein and Zappettini, 2015).

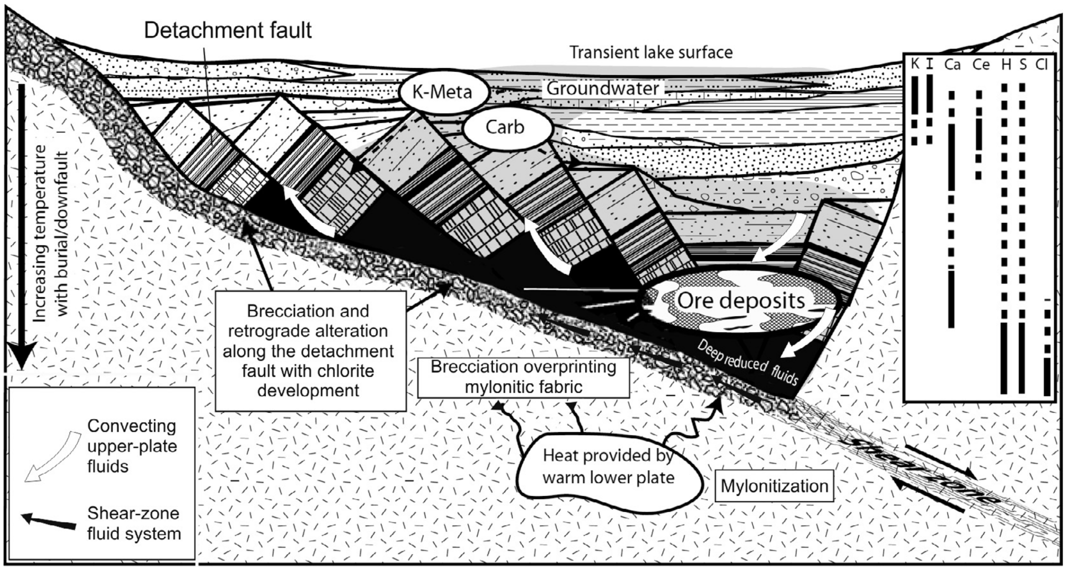

Fig. 5. Idealized model of hydrothermal alteration types associated with a detachment zone (modified from Michalski et al., 2007). Alteration types zoning: potassium metasomatism (K), sericitization (I), carbonatization (Ca), Celadonite (Ce), hematititization (He), silicification (S), chloritization (Cl).

Table 2
Types of deposits related to areas of rifting and associated hydrothermal alteration.

Deposit model	Hydrothermal alteration
Se-rich polymetallic	Carbonatization, hematitization, slight propylitization
Five elements polymetallic	Chloritization, carbonatization, argilization, hematitization
Simple polymetallic	Phyllic: sericitization, silicification, piritization
Fluorite and barite veins	Phyllic: sericitization, silicification
Mn veins	Carbonatization, silicification, caolinization
Cu-Au in detachment-fault zones	Pre-mineralization K-Metasomatism: adularitization Propylitic: Carbonatization, chloritization Sericitization (illite) Hematitization. Celadonite in basaltic levels

The study of the Artillery Mountains District (Arizona, USA) allowed establishing a model of remobilization of Mn from sedimentary sequences, although the relationship with basalts whose chemistry is consistent with a possible source of Mn is not ruled out. In this context, the presence of low temperature K metasomatism, linkable with alkaline brines, could provide a mechanism for release and mobilization of Mn (Derby, 2012).

3.5.3. Selenium

There are limited studies regarding the availability and release mechanisms of Se from geological sources in a fluid medium. The similarity of Se and S results in the replacement of S by Se in rocks with sulfides (Matamoros-Veloza et al., 2011), which can be leached as a result of oxidation of sulfides, being the release mechanisms favored in alkaline environments (Dixon, 2007).

In seawater, 80% of the dissolved Se is concentrated as organic selenides in depths less than 300 m (Cutter and Bruland, 1984). These data are consistent with the concentration of Se in black shales of marine basins enriched in metals, with measured values of 40 ppm (Daba Region, China, Kunli et al., 2003) and up to 300 ppm (Training Phosphoria, Western Phosphate Resource Area, USA, Ryser et al., 2005). The Se in these sediments is associated with both organic matter and Fe sulfides, the latter with contents of up to 0.2% Se (Ryser et al., 2005). Se has also been identified as selenite and selenate, forming adsorption complexes in Fe oxides and clays, being this the most easily leachable source (Ryan and Dittrick, 2001).

3.5.4. Fluorine

The source of fluorine has been subject of debates and different origins have been proposed to explain the formation of large fluorite districts in the world. Fluorine occurs in rift environments in anomalous amounts, and, in this context, Van Alstine (1976) highlighted its relationship with volcanic systems involving acid alkaline magmatism. However, Seager et al. (1984) demonstrated that there is a coincidence between the fluorite mineralization age and the age of mafic alkaline magmatic episodes.

Tropper and Manning (2007) performed fluorite solubility studies which indicated that the solubility of this mineral is low to moderate in water above 600 °C and very soluble in the water-NaCl system, suggesting that in metamorphic and igneous environments in the lower crust, saline fluids can be enriched in fluorine from pre-existing fluorite.

Furthermore, isotopic data of fluid inclusions in fluorite indicate the presence of Cl of asthenospheric origin (Partey, 2004). Given that Cl and F have a similar chemical behavior during the degassing of magma (Thordarson et al., 1995), Partey (2004) considered a mantle source for fluorine, in coincidence with the model proposed by Plumlee et al. (1995). Indeed, considering the limited depth of the burial of acidic volcanics in rift sequences and the P-T conditions required to solubilize fluorite, these can be disregarded as the main source of fluorine.

3.5.5. Barium

In the deposits analyzed above, Ba is considered to be concentrated from the leaching of marine sedimentary sequences. In marine sediments, Ba is associated with several phases, including organic matter, carbonates, opal, Fe-Mn oxyhydroxides, silicates and other terrestrial detrital material (Dehairs et al., 1980). In this environment, the contribution of Ba released in cold seeps along fault scarps is important and equivalent to biogenic Ba proportions (Torres et al., 2002).

The fluids of meteoric origin chemically evolve at depth, producing sulfate-rich brines. This process facilitates the mobilization of Ba, Pb and other metals; however, in some cases, mixing with formational waters and even with magmatic fluids is not ruled out (McLemore et al., 1998). Fluid inclusion studies, isotopic data and structural information allow disregarding the relationship between Ba and exhalative sources in several mining districts (Kontak et al., 2006).

4. Regional metallogenic model

Detachment zones are extensional faults with displacements that can reach several tens of kilometers. They have been explained as a product of evolution of shear zones that controlled low-angle extensional crustal lithospheric processes at high levels (Wernicke, 1981; Spencer and Reynolds, 1989). In these areas, the associated processes of brecciation, retrograde metamorphism in the lower block and juxtaposition with non-metamorphosed upper block rocks, are common. Detachment zones are usually associated at shallow levels with pull-apart complexes and closely spaced sets of normal faults (Davis and Lister, 1988).

Two different geotectonic environments of metallogenic interest, involving extensional faults associated with detachment zones in depth, can be identified:

1) Continental extension in a back-arc setting: this occurs in a tectonic context of negative roll-back, which favors a rise of the asthenospheric mantle to shallow levels and generates a potential source of heat that can induce melting in the lithosphere (Lips, 2002). Examples of this setting are the Shadow Valley, Chemehuevi and Artillery basins in the southwest of the U.S. Cordillera (Friedmann and Burbank, 1995). In the back-arc of the Gondwanan arc in South America, the rift geometry is usually controlled by the reactivation of older structures (e.g. Cuyo Basin, Ramos and Kay, 1991), being common the presence of bimodal volcanism (e.g. Neuquén Basin, Franzese, 2007). In the shallow levels of this environment, Se-rich polymetallic, simple Ag-Pb-Zn, five-element, barite and fluorite veins occur. The deep alkaline magma linked to the rifting process can be the source of F and Mn, which, once collected by the fluids circulating along direct faults associated with the detachment zones, generate veins of these elements.
2) Extension with rift development and production of oceanic crust in a passive continental margin: the early stages of continental breakup are characterized by normal faulting and development of rift systems, with related tholeiitic and alkaline dikes and basalt flows, bimodal magmatic suites and, locally, Na- and K-rich magmatic rocks and carbonatites. Two mechanisms can lead to this type of rifting (Ruppel, 1995): a) an active mechanism in which hot mantle plumes or diapirs initiate the rifting process associated with predominantly extensive alkaline volcanism (e.g. East African Rift, Furman et al., 2016 and references therein); and b) a passive mechanism related to lithospheric extension where a lithospheric scale detachment is involved; such is the case of the Rhine Graben (Lopes Cardoso and Granet, 2003), where Pb-Zn, Mn, fluorite and barite deposits occur (Fusswinkel et al., 2013).

In the pre-breaking stage of the continent, the continental crust is under extensional stress and becomes thinner, originating half-grabens related to detachment zones. The extension accompanied by a displacement along a main detachment zone causes a non-uniform extension of the crust and the lithosphere (Becker et al., 2014). In this environment, extensive rhyolitic magmatism of crustal origin develops (e.g. Marifil Formation in the Argentine epicontinental margin and Whitsunday Volcanic Province in the Eastern Australia passive margin, Bryan et al., 2000) and fluorite and Mn mineralizations occur.

Based on the analysis performed on mineral deposits linked to faults in an extensional context presented in this paper, we propose to group mineral deposits into three environments that represent different exposure levels:

1) Mineral deposits in the environment of detachment faults. This group includes Cu-Au, Au-Ag and Pb-Zn-Ag polymetallic vein-type, stockwork and replacement deposits and the non-magmatic end-member of the IOCG model.

2) Mineral deposits associated with high-angle direct faults.

2a) Associated with half-grabens:

i. In areas where the upper block involves felsic (e.g. dominant rhyolitic) magmatism. This group includes fluorite and Mn veins.
ii. In areas where the upper block and the sedimentary sequence filling the half-grabens have associated mafic magmatism (diabase, tholeiitic basalts). This group includes Se-rich polymetallic veins and simple Pb-Zn-Ag veins.

2b) Associated with direct faults that are not linked with half-grabens in areas where the upper block consists of a sedimentary or metasedimentary basement. This group includes five-element veins (with or without U), simple Pb-Ag-Zn veins and barite veins, whose composition is determined by the availability of elements leached by fluids of metamorphic or metamorphic-sedimentary origin.

3) Mineral deposits associated with sedimentary sequences filling half-grabens. This group includes lacustrine Mn deposits and stratabound barite deposits. Typical polymetallic SEDEX (Pb-Ag-Zn) and stratabound Cu, Cu-Co and Cu-U-V deposits also fall into this group, although they have not been described in this paper because there is no specific relationship with detachment-related extension.

Fig. 6 shows the generalized conceptual metallogenic model defined from the parameters analyzed.

5. Discussion

The analysis of the different tectonic settings described and of the various types of mineral systems associated with detachment zones allows highlighting some interesting similarities and differences. Deposits related to continental extension in a back-arc setting, where the upper block consists of a sedimentary or metasedimentary basement sequence, tend to be richer in chalcophile elements. On the other hand, if the upper block involves felsic (e.g. dominant rhyolitic) magmatism, F, Mn and Fe deposits tend to be formed.

These differences can be explained in terms of oxygen fugacity and S availability, which govern transport and precipitation of metals dissolved in the mineralizing fluids, as analyzed by Barton and Johnson (2000). Increasing chlorine (and fluorine) increases the solubility and transport of many elements; high-salinity fluids (such as brines) or fluorine-rich deep-seated fluids can transport metals more effectively than dilute fluids (Pirajno, in press). On the other hand, since S is essential to precipitate many metals, particularly the chalcophile elements including Cu, Zn, Pb and Se, the S content limits the amount of metals to be precipitated. In contrast, siderophile and lithophile elements, such as Fe, Mn, REE, P and U, form oxides, phosphates and carbonates and thus do not depend on the S concentrations. In an oxidized environment, rich-chlorine or rich-fluorine and poor-S fluids will precipitate Fe-oxide-rich parageneses; if there is enough S in a reduced environment, chalcophile sulfides will form. Also, the origin of fluids needs

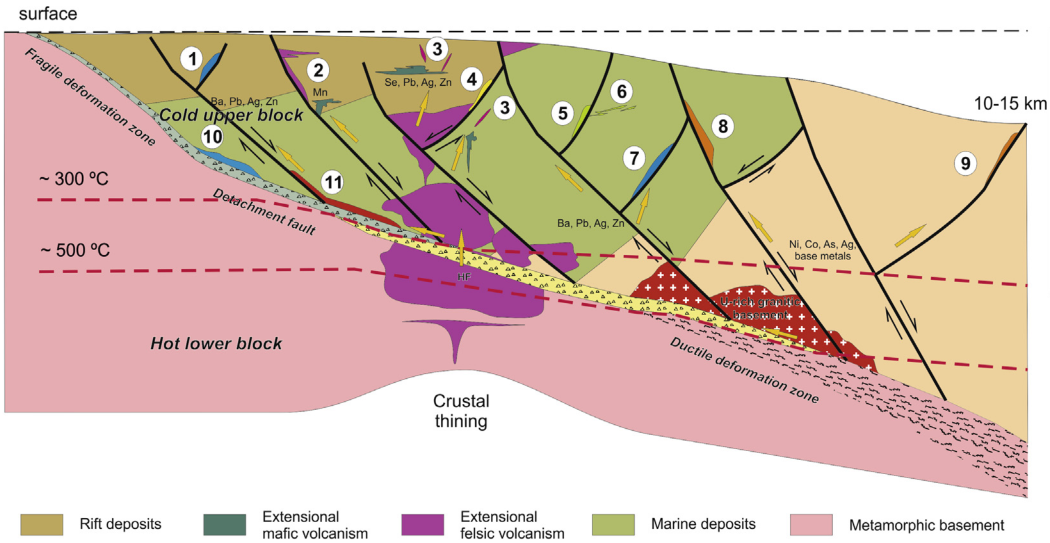

Fig. 6. Generalized model of rift-related deposits. 1. Simple Ag-Pb-Zn veins. 2. Mn veins and lacustrine Mn. 3. Se-rich polymetallic veins. 4. Fluorite veins. 5. Barite veins. 6. Stratabound barite. 7. Five-element-U veins. 8. Five-element veins. 9. Carbonate replacements. 10. Cu-Au-Fe replacements, breccias and veins.

to be considered: magmatic fluids are usually enriched in S, whereas, in non-magmatic fluids, the S content depends on the S availability in the leached sedimentary sequence.

IOCG deposits related to non-magmatic fluids constitute Fe-oxide-rich, sulfide-poor REE-Cu-Co-Au-Ag-bearing mineralization. Mn veins form in a similar setting. In an oxidizing environment, the available Mn in manganous soluble forms is converted into insoluble manganic forms. Fe^{+2} and Mn^{+2} can also be oxidized by chlorine, forming ferric hydroxide and MnO_2. MnO_2 also precipitates when reducing deep waters enriched in dissolved Mn^{+2} and Fe^{+2} well up on the shallow region and mix with oxygenated surface water above the redox interface. Extreme Fe fractionation is caused by a low solubility of Fe in low Eh environments where Fe precipitates as Fe sulfide. A subsequent increase in Eh and/or pH of Mn-rich water may produce Mn-rich, Fe-depleted ores. Fluorine deposits also prevail in this setting, where bimodal dominantly rhyolitic volcanic rocks are widespread.

Barton and Johnson (2000) describes a modern example, the Salton Trough rift basin, where active bimodal magmatism drives the circulation of brines (originated from the evaporites of the basin), and forms Fe-oxide-(Cu-Au-REE-Co-Ag-U)-bearing veins, while Pb and Zn remain in solution because of the limited S content. Associated alteration minerals vary with depth, from shallow (carbonate-illite-chlorite ± K-feldspar) to intermediate (biotite ± chlorite ± K-feldspar ± actinolite) and deep (salite-actino lite-oligoclase-biotite-andradite) assemblages.

Conversely, Cu ± Pb ± Zn ± Ag ± Au ± Co ± Se mineralizations developed at the top of detachment fault systems (as well as polymetallic sedimentary exhalative deposits resulting from dewatering of major sedimentary basins along normal faults) result from the mixing of hot, reduced, S-rich, metal-bearing ascending fluids (controlled by the large-scale fault-zone architecture) with cold high-level oxidized fluids.

6. Conclusions

From a metallogenic point of view, the rift environment analyzed is characterized by a group of different deposit models, whose presence can, in turn, be a useful tool to identify this geodynamic environment. The paragenesis of the different deposit types is conditioned by the level of exposure and the lithology involved, both in the lower and the upper blocks, as well as by the filling of the basins. In addition, the degree of development of the rift and the geodynamic context determine the presence or absence of magmatism and its geochemical characteristics, with the resulting metallogenic implications.

The economic importance of the detachment-related deposits described in a continental rift setting is mainly related to industrial minerals. Locally, detachment-related Au deposits as well as Cu-Au IOCG-type deposits could be found, increasing the economic potential of this extensional setting. The rift environment itself, although not necessarily related to detachments, may have significant economic importance, since it hosts polymetallic SEDEX deposits, stratabound Cu-Co and Cu-U-V deposits and Algoma-type BIMFs. If deposits directly related to magmatic activity (e.g. diamond kimberlites, REE-bearing carbonatites and low-sulfidation Au-epithermal deposits) are also considered, the economic importance of this setting is significantly increased.

References

Aliotta, G., 1999. Yacimientos de fluorita de Río Negro y Chubut. In: Zappettini, E.O. (Ed.), Recursos Minerales de la República Argentina, Anales 35, pp. 1239–1247.

Austin, J.R., Gazley, M.F., Walshe, J.L., Godel, B., le Gras, M., Patterson, B.O., 2016. UNCOVER Cloncurry – The Monakoff Cu-Au-U Deposit: Integrated Petrophysical and Geochemical Analyses. CSIRO, Australia.

Baatarstog, B., 2006. Fluid inclusion and stable isotope studies of hydrothermal vein deposits, Schwarzwald, Germany (PhD. Thesis), Fakultät der Eberhard-Karls-Universität Tübingen, Tübingen, Germany.

Barton, M.D., 2014. Iron Oxide (-Cu-Au-REE-P-Ag-U-Co) Systems. In: Holland, H., Turekian, K. (Eds.), Treatise on Geochemistry, second ed., vol. 13, pp. 515–541.

Barton, M.D., Johnson, D.A., 2000. Alternative brine sources for Fe-Oxide(-Cu-Au) systems: implications for hydrothermal alteration and metals. In: Porter, T.M. (Ed.), Hydrothermal Iron Oxide Copper-Gold & Related Deposits: A Global Perspective. Australian Mineral Foundation, Adelaide, pp. 43–60.

Beaudoin, G., Sangster, D.F., 1992. A descriptive model for silver-lead-zinc veins in clastic metasedimentary terranes. Econ. Geol. 87, 1005–1021.

Becker, K., Franke, D., Trumbull, D., Schnabel, D., Heyde, I., Schreckenberger, B., Koopmann, H., Bauer, K., Jokat, W., Krawczyk, C.M., 2014. Asymmetry of high-velocity lower crust on the South Atlantic rifted margins and implications for the interplay of magmatism and tectonics in continental breakup. Solid Earth 5, 1011–1026.

Bennett, E.H., Venkatakrishnan, R., 1982. A palinspastic reconstruction of the Coeur d'Alene mining district based on ore deposits and structural data. Econ. Geol. 77, 1851–1866.

Berry, L.G., Petruk, W., 1971. The Silver-Arsenide Deposits of the Cobalt-Gowganda Region, Ontario. Mineralogical Association of Canada, Quebec.

Bjerkgård, T., 2012. N008 Kongsberg Ag and N010 Modum Co-As-Au-Ag. In: Geological Survey of Finland (Ed.), Mineral deposits and metallogeny of Fenoscandia, Spec. Pap. 53, pp. 56–61.

Brodtkorb, M.K., 1999. Los distritos seleníferos de La Rioja. In: Zappettini, E. O. (Ed.), Recursos Minerales de la República Argentina, Anales 35, pp. 625–629.
Brodtkorb, M.K., Crosta, S., 2010. Reseña de la ubicación geográfica de los seleniuros de la sierra de Umango, provincia de La Rioja. Rev. Asoc. Geol. Argent. 67 (2), 272–277.
Brodtkorb, M.K., Etcheverry, R., 2000. Edad K/Ar dela mineralización de manganeso de Aguada del Monte, provincia de Córdoba. Rev. Asoc. Geol. Argent. 55, 280–283.
Brodtkorb, M.K., Paar, W., 2013. Sobre los minerales presentes en el yacimiento selenífero de Cacheuta. 12 Congreso de Mineralogía y Metalogenia, Extended Abstracts, pp. 25–28.
Bryan, S., Ewart, A., Stephens, C.J., Parianos, J., Downes, P.J., 2000. The Whitsunday Volcanic Province, Central Queensland, Australia: lithological and stratigraphic investigations of a silicic-dominated large igneous province. J. Vol. Geotherm. Res. 99, 55–78.
Cabral, A.R., Lehmann, B., 2007. Seleniferous minerals of palladium and platinum from Ouro Preto-bearing mineralization in Brazil. Ore Geol. Rev. 32. 681-81.
Cabral, A.R., Lehmann, B., Kwitko, R., Cravo Costa, C.H., 2002. The Serra Pelada Au–Pd–Pt deposit, Carajás mineral province, northern Brazil: Reconnaissance mineralogy and chemistry of very high grade palladian gold mineralization. Econ. Geol. 97, 1127–1138.
Cabral, A.R., Koglin, N., Braetz, H., 2012. Gold-bearing ferroselite ($FeSe_2$) from Trogtal, Harz, Germany, and significance of its Co/Ni ratio. J. Geosciences 57, 265–272.
Canals, A., Cardellach, E., 1996. Caracterización de los fluidos en sucesivas fases de fracturación en las Cadenas Costero Catalanas y su registro en los filones de Ba-F de baja temperatura. Geogaceta 20 (3), 696–699.
Cardó, R., 1999. Distrito polimetálico Castaño Viejo, San Juan. In: Zappettini, E.O. (Ed.), Recursos Minerales de la República Argentina, Anales 35, Buenos Aires, pp. 857–863.
Carrasquero, S., Rubinstein, N., Bevins, R., 2013. Paragénesis mineral de la veta Tajo, Yacimiento Paramillos de Uspallata, Mendoza. Argentina. Acta Geol. Llilloana 25 (1–2), 3–8.
Castillo, A. L., 1999. Depósitos de baritina de Cordillera Oriental, Salta. In: Zappettini E. O. (Ed.), Recursos Minerales de la República Argentina, Anales 35, pp. 499–503.
Centeno, R., Rosas, M., Rubinstein, N., 2009. Carta Minero-Metalogenética 3569-IV Embalse El Nihuil, Provincia De Mendoza. Servicio Geológico Minero Argentino, Buenos Aires.
Cicciarelli, M.I., 1990. Análisis estructural del sector oriental del Macizo Nordpatagónico y su significado metalogénico. Unpublished (PhD thesis), Universidad Nacional de La Plata, La Plata, Argentina.
Clark, S., Orris, G.J. 1991. Descriptive model of epigenetic vein barite. In: Orris, G.J., Bliss, J.D. (Eds.), Some Industrial Mineral Deposit Models: Descriptive Deposit Models, U.S. Geological Survey Open-file Report 91–11A, pp. 24–25.
Clark, A.M., Criddle, A.J., Fejer, E.E., 1974. Palladium arsenide-antimonides from Itabira, Minas Gerais. Brazil. Mineral. Mag. 39, 528–543.
Constantopoulos, J., 1988. Fluid inclusions and Rare Earth element geochemistry of fluorite from South-Central Idaho. Econ. Geol. 83, 626–636.
Cutter, G.A., Bruland, K.W., 1984. The marine biochemistry of selenium: a re-evaluation. Limnol. Oceanogr. 29, 1179–1192.
Davis, G., Lister, G.S., 1988. Detachment faulting in continental extension; perspectives from the Southwestern U.S. Cordillera. Geol. Soc. Am. Special Pap. 218, 133–159.
Dehairs, F., Chesselet, R., Jedwab, J., 1980. Discrete suspended particles of barite and the barium cycle in the open ocean. Earth Planet. Sci. Lett. 49, 528–550.
Derby, S. 2012. Depositional modes of manganese oxides at Artillery Peak, Mohave County, Arizona. MSG thesis, Nevada University. Available from: http://data.nbmg.unr.edu/.
Dixon, B.M., 2007. Selenium in geological samples: investing in a mathematical mystery. In: British Columbia 31st. Annual Mine Reclamation Symposium. Available from: http://hdl.handle.net/2429/8488.
Drake, W.R., 2005. Structural analysis, stratigraphy, and geochronology of the San José Island accommodation zone, Baja California Sur, Mexico (M Sc Thesis). Northern Arizona University, Arizona.
Duncan, J.T., 1990. The geology and mineral deposits of the Northern Plomosa District. La Paz County, Arizona, Arizona Geological Survey Open File Report, 90–110.
Eggleston, T.L., Norman, D.I., Chapin, Ch.E., Savin, S. 1983. Geology, alteration and genesis of the Luis López Manganese District, New Mexico. Guidebook. In: 34th field conference new mexico geological society, pp. 241–246.
El Ghorfi, M., Oberthür, T., Melcher, F., Lüders, V., El Boukhari, A., Maacha, L., Ziadi, R., Baoutoul, H., 2006. Gold–palladium mineralization at Bleïda Far West, Bou Azzer–El Graara Inlier, Anti-Atlas, Morocco. Miner. Deposita 41, 549–564.
Fauqué, L., Caminos, R., 2006. Hoja Geológica 2969-II, Tinogasta, Provincias De La Rioja, Catamarca y San Juan. Servicio Geológico Minero Argentino, Buenos Aires.
Förster, H.J., Cooper, M.A., Roberts, A.C., Stanley, C.J., Criddle, A.J., Hawthorne, F.C., Laflamme, J.H.G., Tischendorf, G., 2003. Schlemaite, (Cu, Ag)6(Pb, Bi)Se4, a new mineral species from Niederschlema – Alberoda, Erzgebirge, Germany: description and crystal structure. Can. Mineral. 41, 1433–1444.
Förster, H.J., Rhede, D., Tischendorf, G., 2004. Mineralogy of the Niederschlema – Alberoda U-Se–polymetallic deposit, Erzgebirge, Germany. i. jolliffeite, NiAsSe, the rare Se-dominant analogue of gersdorffite. Can. Mineral. 42, 841–849.
Franzese, J.R., 2007. Estratigrafía de "sin-rift" (Triásico Superior-Jurásico Inferior) de la Cuenca Neuquina en la Sierra de Chacaico, Neuquén, Argentina. Rev. Asoc. Geol. Chile 34 (1), 49–62.
Friedmann, S.J., Burbank, D.W., 1995. Rift basins and supradetachment basins: intracontinental extensional endmembers. Basin Res. 7, 109–127.
Furman, T., Nelson, W.R., Elkins-Tanton, L.T., 2016. Evolution of the East African rift: Drip magmatism, lithospheric thinning and mafic volcanism. Geochim. Cosmochim. Acta 185, 418–434.
Fusswinkel, T., Wagner, T., Wälle, M., Wenzel, T., Heinrich, C., Markl, G., 2013. Fluid mixing forms basement-hosted Pb-Zn deposits: Insight from metal and halogen geochemistry of individual fluid inclusions. Geology 41, 679–682.
Garrido, M., Domínguez, E., Schalamuk, I., 2001. Veta Tajo, Paramillos de Uspallata, Mendoza. Características del sistema hidrotermal. Rev. Asoc. Geol. Argent. 56, 99–110.
Gilder, S.A., Keller, G., Luo Ming, R., Goode, P.C., 1991. Eastern Asia and the Westem Pacific. Timing and spatial distribution of rifting in China. Tectonophysics 197, 225–243.
Grainger, C.J., Groves, D.I., Tallarico, F.H.B., Fletcher, I.R., 2008. Metallogenesis of the Carajás Mineral Province, Southern Amazon Craton, Brazil: varying styles of Archean through Paleoproterozoic to Neoproterozoic base- and precious-metal mineralisation. Ore Geol. Rev. 33, 451–489.
Grundmann, G., Lehrberger, G., Schnorrer-Köhler, G., 1990. The El Dragon mine, Potosi. Bolivia. Mineral. Rec. 21, 133–150.
Guiraud, R., 1998. Mesozoic rifting and basin inversion along the northern African Tethyan margin: an overview. In: Macgregor, D.S., Moody, R.T.J., Clark-Lowes, D. D., (Eds), Petroleum geology of North Africa, Geol. Soc. Lond. Spec. Publ. 132, London.
Higueras, P., Oyarzun, R., Lunar, R., Sierra, J., Parras, J., 1999. The Las Cuevas deposit, Almaden district (Spain): An unusual case of deep-seated advanced argillic alteration related to mercury mineralization. Miner. Deposita 34, 211–214.
Higueras, P., Munhá, J., Oyarzun, R., Tassinari, C.C.G., Ruiz, I.R., 2005. First lead isotopic data for cinnabar in the Almadén district (Spain): implications for the genesis of the mercury deposits. Geogaceta 37, 67–70.
Hora, Z. D. 1996a. Vein Fluorite-barite, in Selected British Columbia Mineral Deposit Profiles. In: Lefebure, D.V., Höy, T. (Eds.), Metallic Deposits, vol. 2. British Columbia Ministry of Employment and Investment, pp. 85–88 (Open File 1996–13).
Hora, Z.D., 1996b. Vein Barite. In: Lefebure, D.V., Höy, T. (Eds.). Selected British Columbia mineral depost profiles, vol. 2. British Columbia ministry of employment and investment, pp. 81–84 (Open File 1996–13).
Hutton, L.J., Denaro, T.J., Dhnaram, C., Derrick, G.M., 2012. Mineral Systems in the Mount Isa Inlier. Episodes 35 (1), 120–130.
Jessey, D.R., 2010, Geology and ore genesis of the Calico Mining District, in Overboard in the Mojave. California Desert Studies Symposium-2010, pp. 213–223.
Johan, Z., Picot, P., Ruhlmann, F., 1982. Paragenetic evolution of the Uranium Mineralization Rich in Selenides at Chaméane (Puy-de-Dome) France: Chaméanite, Geffroyite and Giraudite, Three New Selenides of Cu, Fe, Ag and As. Tschermaks Min. Petrog. Mitt. 29, 151–167.
Johan, Z., Picot, P., Ruhlmann, F., 1987. The ore mineralogy of the Otish Mountains uranium deposit, Quebec: skippenite, Bi_2Se_2Te, and watkinsonite, $Cu_2PbBi_4(Se,S)_8$, two new mineral species. Can. Mineral. 25, 625–638.
Kissin, S.A., 1992. Five-element (Ni-Co-As-Ag-Bi) veins. Geoscience Can. 19 (3), 113–124.
Kleiman, L.E., Japas, M.S., 2009. The Choiyoi volcanic province at 34 S–36 S (San Rafael, Mendoza, Argentina): implications for the Late Palaeozoic evolution of the southwestern margin of Gondwana. Tectonophysics 473, 283–299.
Kontak, D.J., Kyser, K., Gize, A., Marshall, D., 2006. Structurally controlled vein barite mineralization in the maritimes basin of eastern canada: geologic setting, stable isotopes, and fluid inclusions. Econ. Geol. 101, 407–430.
Kríbek, B., Zák, K., Dobes, P., Leichmann, J., Pudilová, M., René, M., Scharm, B., Scharmová, M., Hájek, A., Holeczy, D., Hein, U.F., Lehmann, B., 2009. The Rožná uranium deposit (Bohemian Massif, Czech Republic): shear zone-hosted, late Variscan and post-Variscan hydrothermal mineralization. Mineral. Deposita 44, 99–128.
Kunli, L., Lirong, X., Jian'an, T., Douhu, W., Lianhua, X., 2003. Selenium source in the selenosis area of the Daba region, South Qinling Mountain, China. Environ. Geol. 45, 426–432.
Leal, P.R., Correa, M.J., Ametrano, S.J., Etcheverry, R.O., Brodtkorb, M.K., 2008. The manganese deposits of the Pampean Ranges, Argentina. Can. Mineral. 46, 1215–1233.
Lefebure, D.V., 1996. Five-element veins Ag-Ni-Co-As±(Bi, U). In: Lefebure, D.V., Höy, T. (Eds.), Selected British Columbia mineral deposit profiles, vol. 2, British Columbia ministry of employment and investment, pp. 89–91 (Open File 1996–13).
Lindgren, W., 1928. Mineral Deposits. Mc Graw-Hill, New York.
Lips, A.L.W., 2002. Correlating magmatic-hydrothermal ore deposit formation over time with geodynamic processes in SE Europe. In: Blundell, D.J., Neubauer, F., Von Quadt, A. (Eds.) The Timing and Location of Major Ore Deposits in an Evolving Orogen, Geol. Soc. Lond. Spe. Pub. 204, pp. 69–79.
Long, K.R., 1992a. Preliminary descriptive deposit model for detachment-fault-related mineralization. In: Bliss, J. (Ed.), Developments in Mineral Deposit Modeling. U.S. Geological Survey Bulletin 2004, pp. 52–56.
Long, K.R., 1992b. Preliminary descriptive deposit model for detachment-fault-related mineralization. In: Bliss, J. (Ed.), Developments in Mineral Deposit Modeling. U.S. Geological Survey Bulletin 2004, pp. 57–62.
Lopes Cardoso, G.G.O., Granet, M., 2003. New insight in the tectonics of the southern Rhine Graben-Jura region using local earthquake seismology. Tectonics. http://doi:10.1029/2002TC001442.

López, L., 2011. Geología y metalogénesis del distrito polimetálico Purísima-Rumicruz, departamento de Cochinoca, Provincia de Jujuy, Argentina. Unpublished PhD thesis, Universidad Nacional de La Plata, La Plata, Argentina.
Mallimacci, H., Caripo, F., Rubinstein, N., 2010. Carta Minero-Metalogenética 3769-II Agua Escondida, Provincias De Mendoza Y La Pampa. Servicio Geológico Minero Argentino, Buenos Aires.
Malvicini, L., Delpino, D., 1989. Metalogénesis de los complejos riolíticos de la provincia geológica sanrafaelino pampeana y la comarca norpatagónica, Argentina. Procesos metalogenéticos. Ser. Correl. Geol. 3, 63–82.
Marchev, P., Singer, B.S., Jelev, D., Hasson, S., Moritz, R., Bonev, N., 2004. The Ada Tepe deposit: a sediment-hosted, detachment fault-controlled, low-sulfidation gold deposit in the Eastern Rhodopes, SE Bulgaria, Schweiz. Mineral. Petrogr. Mitt. 84, 59–78.
Masson, D.G., Miles, P.R., 1983. The development of mesozoic sedimentary basins around the margins of the north atlantic and their hydrocarbon potential. Internal Document No. 195, Institute of Oceanographic Sciences.
Matamoros-Veloza, A., Newton, R.J., Benning, L.G., 2011. What controls selenium release during shale weathering? Appl. Geochem. 26, S222–S226.
Mats, V.D., Perepelova, T.I., 2011. A new perspective on evolution of the Baikal Rift. Geosci. Front. 2 (3), 349–365.
McLemore, V.T., Giordano, T.H., Lueth, V.W., Witcher, J.C., 1998. Origin of Barite Fluorite-Galena Deposit in the Rio Grande Rift, New Mexico, Guidebook 49. New Mexico Geological Society, Socorro, U.S..
McPhie, J., Kamenetsky, V., Allen, S., Ehrig, K., Agangi, A., Bath, A., 2011. The fluorine link between a supergiant ore deposit and a silicic large igneous province. Geology 39 (11), 1003–1006.
Michalski, J.R., Reynolds, S.J., Niles, P.B., Sharp, T.G., Christensen, P.R., 2007. Alteration mineralogy in detachment zones: Insights from Swansea, Arizona. Geosphere 3 (4), 184–198.
Milanovsky, E.E., 1983. Major stages of rifting evolution in the Earth's history. Tectonophysics 94, 599–607.
Morata, D., Higueras, P., Dominguez- Bella, S., Parras, J., Velasco, F., Aparicio, P., 2001. Fuchsite and other Cr- rich phyllosilicates in ultramafic enclaves from the Almaden mercury mining district, Spain. Clay Miner. 36, 345–354.
Morello, O., Rubinstein, N., 1997. Mineralización de As-Ni-Co-U-Bi de la manifestación nuclear Carrizal, provincia de San Juan, Argentina. Rev. Asoc. Geol. Argent. 52 (1), 41–46.
Morello, O., Rubinstein, N., Hongn, F., Ferreira, L., Anesa, J., Arias, A., 2011. Modelo Metalogenético del Depósito de Uranio, Las Termas, Fiambalá, Catamarca, Argentina. Bol. Geol. Min. 122 (3), 325–332.
Mumin, A.H., Corriveau, L., Somarin, A.K., Ootes, L., 2007. Iron oxide copper–gold-type polymetallic mineralization in the Contact Lake Belt, Great Bear Magmatic Zone, Northwest Territories, Canada. Explor. Min. Geol. 16, 187–208.
Nickel, E.H., 2002. An unusual occurrence of Pd, Pt, Au, Ag y Hg minerals in the Pilbara region of western Australia. Can. Mineral. 40, 419–433.
Oden, M.I., 2012. Barite Veins in the Benue Trough: Field Characteristics, the Quality Issue and Some Tectonic Implications. Environ. Nat. Resour. Res. 2 (2), 21–31.
Paiement, J.Ph., Beaudoin, G., Paradis, S., Ullrich, T., 2012. Geochemistry and Metallogeny of Ag-Pb-Zn Veins in the Purcell Basin, British Columbia. Econ. Geol. 107, 1303–1320.
Palero-Fernández, F.J., Martin-Izard, A., Zarzalejos Prieto, M., Mansilla-Plaza, L., 2015. Geological context and plumbotectonic evolution of the giant Almadén mercury deposit. Ore Geol. Rev. 64, 71–88.
Pankhurst, R.J., Riley, T.R., Fanning, C.M., Kelley, S.R., 2000. Episodic silicic volcanism along the proto-Pacific margin of Patagonia and the Antarctic Peninsula: plume and subduction influences associated with the break-up of Gondwana. J. Petrol. 41, 605–625.
Partey, F., 2004. Source of Fluorine and Petrogenesis of the Rio Grande Rift Type Barite-Fluorite-Galena Deposits (MSc. Thesis). Miami University, Miami.
Pešek, J., Holub, V., Jaroš, J., Malý, L., Martínek, K., Prouza, V., Spudil, J., Tásler, R., 2001. Geology and Mineral Deposits of the Upper Palaeozoic Limnic Basins of the Czech Republic. Czech Geological Survey, Prague.
Pirajno F., (in press). Halogens in hydrothermal fluids and their role in the formation and evolution of hydrothermal systems, in: Harlov, D., Aranovich, L. (in press). The role of halogens in terrestrial and extraterrestrial geochemical processes: Surface, Crust and Mantle. Lecture Notes in Earth System Sciences, Springer.
Plumlee, G.S., Goldhaber, M.B., Rowan, E.L., 1995. The potential role of magmatic gases in the genesis of Illinois-Kentucky fluorspar deposits: Implications from chemical reaction path modeling. Econ. Geol. 90 (5), 999–1011.
Puritch, E., Bradfield, A., Routledge, R., Sutcliffe, R., Burga, D., Barry, J., Cornejo, F., Batelochi, M., Lister, D., 2016. Technical Report and updated Resource Estimate on the EPP Project. Mato Grosso, Brazil. Aura Minerals Inc. NI 43–101 & 43–101F1 Technical Report.
Ramdohr, P., Schmitt, M., 1955. Vier Neue Natürliche Kobalt Selenide Vom Steinbruch Trogtal Bei Lautenthal Im Harz. Neue Jarbuch Mineralogie, Mh, pp. 133–142.
Ramos, V.A., Aguirre-Urreta, M.B., 2000. Tectonic evolution of the Andes. In: Cordani, U.G., Milani, E.J., Thomaz Filho, A., Campos, D.A. (Eds.), Tectonic Evolution of South America (31st International Geological Congress). Rio de Janeiro, pp. 635–685.
Ramos, V., Kay, S.M., 1991. Triassic rifting and associated basalts in the Cuyo basin, central Argentina. In: Harmon, R.S., Rapela, C.W. (Eds.), Andean Magmatism and its Tectonic Setting, Geol. Soc. Am. Spec. Pap. 265, pp. 79–91.
Reynolds, S.J., Lister, G.S., 1987. Structural aspects of fluid-rock interactions in detachment zones. Geology 15, 362–366.
Roberts, D.G., Bally, A.W., 2012. Regional Geology and Tectonics: Phanerozoic Rift Systems and Sedimentary Basins. Elsevier Sc. Pub, London.
Robertson, A.H.F., 2007. Overview of tectonic settings related to the rifting and opening of Mesozoic ocean basins in the Eastern Tethys: Oman, Himalayas and Eastern Mediterranean regions. In: Karner, G.D., Manatschal, G., Pinheiro, L.M. (eds) Imaging, Mapping and Modelling Continental Lithosphere Extension and Breakup, Geol. Soc. Lond. Spec. Pub. 282, pp. 325–388.
Roddy, M.S., Reynolds, S.J., Smith, B.M., Ruiz, J., 1988. K-metasomatism and detachment-related mineralization, Harcuvar Mountains, Arizona. Geol. Soc. Am. Bull. 100 (10), 1627–1639.
Rodríguez-Díaz, A.A., Blanco-Florido, D., Canet, C., Gervilla-Linare, F., González-Partida, E., Prol-Ledesma, R.M., Morales-Ruano, S., García Vallés, M., 2013. Metalogenia del depósito de manganeso Santa Rosa, Baja California Sur, México. Bol. Soc. Geol. Mexicana 62 (1), 141–159.
Rubinstein, N., Zappettini, E., 2015. Origin and age of rift related fluorite and manganese deposits from the San Rafael Massif, Argentina. Ore Geol. Rev. 66, 334–343.
Ruffell, A., 1998. Characterisation and prediction of sediment-hosted ore deposits using sequence stratigraphy. Ore Geol. Rev. 12 (4), 207–223.
Ruppel, C., 1995. Extensional processes in continental lithosphere. J. Geophys. Res. 100 (B12), 24187–24215.
Ryan, B., Dittrick, M., 2001. Selenium in the Mist Mountain Formation of Southeast British Columbia. British Columbia Geological Survey, Geological Fieldwork 2000, Paper 2001-1, pp. 337-362.
Ryser, A.L., Strawn, D.G., Marcus, M.A., Johnson-Maynard, J.L., Gunter, M.E., Möller, G., 2005. Micro-spectroscopic investigation of selenium-bearing minerals from the Western US Phosphate Resource Area. Geochem. Trans. 6 (1), 1–11.
Sangster, A.L., 2001. Mineral occurrences in the Puna region. Salta and Jujuy provinces, Argentina, Serie Contribuciones Técnicas 16. Servicio Geológico Minero Argentino, Buenos Aires.
Seager, W.R., Shafiqullah, M., Hawley, J.W., Marvin, R.F., 1984. New K-Ar dates from basalts and the evolution of the southern Rio Grande rift. Geol. Soc. Am. Bull. 95, 87–89.
Segal, S., Godeas, M., Pezzutti, N., Zappettini, E. O., 1999. Distrito de plomo, cinc y plata, Pumahuasi, Jujuy. In: Zappettini, E.O. (Ed.), Recursos Minerales de la República Argentina, Anales 35, Buenos Aires, pp. 493–497.
Shepherd, T.J., Bouch, J.E., Gunn, A.G., McKervey, J.A., Naden, J., Scrivener, R.C., Styles, M.T., Large, D.E., 2005. Permo-Triassic unconformity-related Au–Pd mineralisation, South Devon, UK: new insights and the European perspective. Mineral. Deposita 40, 24–44.
Sillitoe, R.H., 2003. Iron oxide–copper–gold deposits: an Andean view. Mineral. Deposita 38, 787–812.
Simon, G., Kesler, S.E., Essene, E.J., 1997. Phase relations among selenides, sulfi des, tellurides, and oxides. II. Applications to Selenide-Bearing Ore Deposits. Econ. Geol. 92, 468–484.
Sizaret, S., Marcoux, E., Bouce, A., Jebrak, M., Stevenson, R., Ellam, R., 2009. Isotopic (S, Sr, Sm/Nd, D, Pb) evidences for multiple sources in the Early Jurassic Chaillac F-Ba ore deposit (Indre, France). Bull. Soc. Géol. France 180 (2), 83–94.
Spalletti, L.A., Fanning, C.M., Rapela, C.W., 2008. Dating the Triassic continental rift in the southern Andes: the Potrerillos Formation, Cuyo Basin, Argentina. Geol. Acta 6, 267–283.
Spencer, J., 1991. The Artillery Manganese District in West – Central Arizona. Arizona Geological Survey, Arizona. Available from: http://www.azgs.az.gov/.
Spencer, J.E. and Reynolds, S.J., 1989. Middle Tertiary Tectonics of Arizona and adjacent areas. In: J.P. Jenny, Reynolds, S.J., (Eds.), Geological Evolution ofArizona, Arizona Geological Society Digest 17, Arizona, pp. 539–574.
Spencer, J.E., Reynolds, S.J., 1992. Mineral Deposits of the Bullard Mineral District, Harcuvar Mountains, Yavapai County, Arizona. Arizona Geological Survey Open-File Report 92-1.
Spencer, J.E., Welty, F.W., 1986. Possible controls of base- and precious-metal mineralization associated with Tertiary detachment faults in the lower Colorado River through, Arizona and California. Geology 14, 195–198.
Spencer, J.E., Duncan, J.T., Burton, W.D., 1988. The Copperstone Mine: Arizona's New Gold Producer. Fieldnotes, vol. 18 (2). Arizona Bureau of Geology and Mining Technology, Arizona, U.S.
Stanley, C.J., Criddle, A.J., Lloyd, D., 1990. Precious and base metal selenide mineralization at hope's Nose, Torquay, Devon. Mineral. Mag. 54, 485–493.
Thordarson, T., Hulsebosch, T., Oskarsson, N., Self, S., 1995. Sulfur, chlorine, and fluorine degassing and atmospheric loading by the 1783–1784 AD laki (Skafttar fires) eruption in Iceland. Bull. Volcanol. 58 (2–3), 205–225.
Tischendorf, G., 1959. Zur genesis einiger Selenidvorkommen, insbesondere von Tilkerode im Harz. Freiberg Forsch, H C69, 1–168.
Torres, M.E., McManus, J., Huh, C., 2002. Fluid seepage along the San Clemente Fault scarp: basin-wide impact on barium cycling. Earth Planet. Sci. Lett. 203, 181–194.
Tropper, P., Manning, C.E., 2007. The solubility of fluorite in H_2O and H_2O–NaCl at high pressure and temperature. Chem. Geol. 242, 299–306.
Van Alstine, R.E., 1976. Continental rifts and lineaments associated with major fluorspar districts. Econ. Geol. 71, 977–987.
Vikre, P.G., 2005. Se-rich precious metal deposits and the significance of Se in sinter, Northern Great Basin. 2005 Salt Lake City Annual Meeting, Extended Abstracts, Paper N 235–8.
Vuorelaine, Y., Huhma, A., Häkli, A., 1964. Sederholmite, wilkmanite, kullerudite mäkinenite and trüstdtite, five new nickel-selenide minerals. CR. Soc. Geol. Finlande 36, 113–125.

Wallis, E., 1994. Erzparagenetische und mineralchemische Untersuchung der Selenide im Harz (Unpubl. Diploma thesis), University of Hamburg, Hamburg, Germany.
Wernicke, B., 1981. Low-angle normal faults in the Basin and Range province; nappe tectonics in an extending orogen. Nature 291, 645–648.
Wilkinson, J.J., 2001. Fluid inclusions in hydrothermal ore deposits. Lithos 55, 229–272.
Wilkinson, W.H., Wendt, C.J., Dennis, M.D., 1988. Gold mineralization along Riverside Mountains Detachment Fault, Riverside County, California. Bulk mineable precious metal deposits of the Western United States, Symposium Proceedings, Part IV, Gold-silver deposits associated with detachment faults, Nevada, pp. 487–504.
Williams, M.R., Holwell, D.A., Lilly, R.M., George, N.D.C., McDonald, I., 2015. Mineralogical and fluid characteristics of the fluorite-rich Monakoff and E1 Cu–Au deposits, Cloncurry region, Queensland, Australia: implications for regional F-Ba-rich IOCG mineralization. Ore Geol. Rev. 64, 103–127.
Zappettini, E.O., Crosta, S., Rubinstein, N., Segal, S., 2015. Revisión De Modelos De Mineralización Asociados a Rifting Implicancias Metalogenéticas Relacionadas Al Rifting Mesozoico En Argentina. Servicio Geológico Minero Argentino, Buenos Aires.
Zartman, R.E., Doe, B.R., 1981. Plumbotectonics-the model. Tectonophysics 75, 135–162.
Ziegler, P.A., Dèzes, P., 2006. Crustal evolution of Western and Central Europe. Geol. Soc., London, Mem. 32, 43–56.
Zorin, Y.A., Turutanova, E.Kh., Mordvinova, V.V., Kozhevnikova, V.M., Yanovskaya, T. B., Treussov, A.V., 2003. The Baikal rift zone: the effect of mantle plumes on older structure. Tectonophysics 371, 153–173.